2011

Band-Pass Filter Feedback System For Use In AM Radio Receivers

Kevin Robert Ford
Lehigh University

Band-Pass Filter Feedback System for Use in AM Radio Receivers

By

Kevin Robert Ford

A Thesis

Presented to the Graduate and Research Committee

of Lehigh University

in Candidacy for the Degree of

Master of Science

in

Electrical Engineering

Lehigh University

28 April, 2011

Thesis is accepted and approved in partial fulfillment of the requirements for the Master of Science in Electrical Engineering.

Band-Pass Filter Feedback System for Use in AM Radio Receivers
Kevin Robert Ford

_____
Date Approved

_____
Douglas R. Frey
Advisor

_____
Filbert J. Bartoli
Department Chair Person

Acknowledgements

My thanks go out to the Lehigh professors who have helped nurture my desire to learn, and helped me learn lessons, both academic and in life that I will keep with me for the rest of my life.

Thanks specifically go out to Professor William Best, my first electrical engineering professor who so enthralled me with his introductory circuits class, the experience motivated me to pursue an Electrical Engineering minor degree as an undergraduate. Thanks to Professor William Haller, who has both been an incredible instructor and mentor and who is responsible for my application to Lehigh University's M.S. Electrical Engineering program.

For all his help in developing and assisting me in the study of this thesis project and for his seemingly limitless patience, my thanks go to Professor Doug Frey. I'll never treat bar napkins the same way after we began drawing circuits on them for fun after class. Thank you for making the hard stuff look easy and explain it in a way that it became easy for me too.

Finally, I thank my family and friends, both at Lehigh and abroad for their support and encouragement through my undergraduate and graduate education at Lehigh.

Table of Contents

List of Tables

List of Figures

List of Symbols and Nomenclature (Alphabetical)

AM ..... Amplitude Modulation

BPF ..... Band-Pass Filter

DFT ..... Discrete Fourier Transform

fdot/f ..... Derivative of f(t) divided by f(t)

LNA ..... Low Noise Amplifier

LO ..... Local Oscillator

LPF ..... Low-Pass Filter

Abstract

Amplitude modulation radio receivers require the use of a core band-pass filter to attenuate both noise and all other radio stations except the station designated by the user. In amplitude modulated signals that use a static band-pass filter, the filter must have a cutoff bandwidth larger than the bandwidth of the input in order to avoid attenuating the desired signal. This thesis proposes that if the core filter is allowed to be time-varying, the filtration process can be improved with the addition of a time-varying feedback system. If such a band-pass filter is used in conjunction with this feedback system, the desired signal will experience almost no attenuation even when the cutoff bandwidth of the filter is significantly sharper. This solution offers potential benefits regarding noise reduction as well.

I. Introduction

A. Background

In a simple AM radio receiver, a low noise amplifier (LNA) acts on an input signal received by an antenna. The output of the LNA is multiplied by a local oscillator (LO1) which demodulates the signal to an intermediate frequency. The band-pass filter which follows the local oscillator stage has its center frequency set at this intermediate frequency. The output of the band-pass filter is multiplied by a second local oscillator (LO2) stage, which demodulates the signal down to the base band. The second local oscillator is followed by a low-pass filter whose job it is to attenuate images of the signal which appear at higher frequencies as a result of the demodulation. The radio receiver system can be represented as the block diagram shown in *Figure 1*.

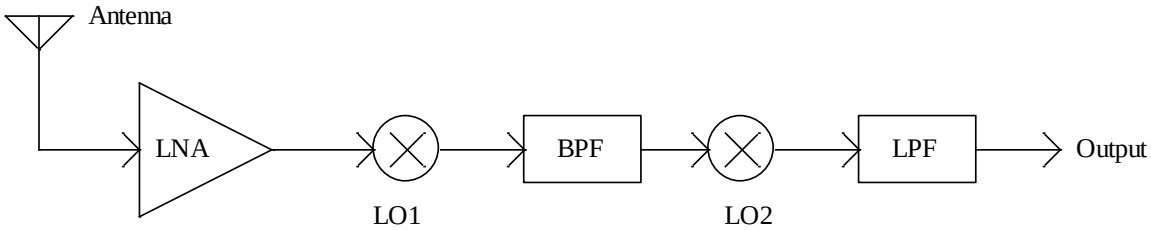

Figure 1: Simple AM Radio Receiver Block Diagram

The input signal after the LNA can be represented as a sinusoidal signal at a relatively high AM radio station frequency multiplied by a signal "f(t)" (in addition to a DC component). This f(t) is the amplitude modulation being applied to the carrier signal. The ideal output of the radio receiver should be just the function f(t) in addition to a DC component, as it is the signal desired by the user.

Allow f(t) to be one which is easily drawn in the frequency domain such as an isosceles triangle. The Fourier transform of the input to the band-pass filter would look

like that shown in *Figure 2*. The triangular sidebands of the signal are the frequency representation of f(t).

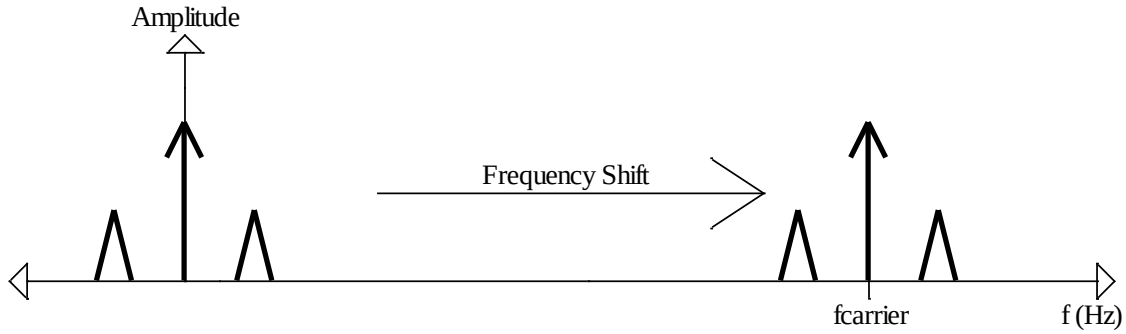

Figure 2: Simple Magnitude Spectrum Plot

The first local oscillator demodulates the signal to an intermediate frequency so before the signal is fed into the band-pass filter. As mentioned before, the carrier frequency ("fcarrier" in *Figure 2*) is demodulated to the same frequency as the center frequency of the band-pass filter. The side bands (drawn in *Figure 2* as simple triangles) remain the same "distance" away from the demodulated carrier frequency as before. As a result, the band-pass filter must be designed so that minimal attenuation of the side bands occurs, as these bands represent the final signal desired by the user. This means that the cutoff bandwidth of the band-pass filter must be rather broad, which also somewhat compromises the filter's ability to filter out undesired signals.

Worse yet, a particularly noisy input may have undesirable levels of noise between the carrier frequency impulse and the side bands. The only way to reject noise between the bands is to sharpen the cutoff bandwidth the band-pass filter, which could result in severe attenuation of the side bands. In order to mitigate the problem of noise between the bands and improve the frequency response of the band-pass filter, a feedback system with gain control may be used. This system will use the output of the band-pass

filter to help reconstruct the sidebands even if the cutoff bandwidth of the filter is narrower of than the signal bandwidth.

B. State Space Approach Applied to the Band-Pass Filter

A common representation for filtering operations is a transfer function using the Laplace operator "s". Equation 1 shows one such representation for a band-pass filter, where ω_o is the center frequency of the filter , and Q is the quality factor or "Q-factor" of the filter. The Q-factor is represented in Equation 2 where $\Delta\omega$ is the 3dB bandwidth of the filter.

(1) $$H(s) = \frac{s\frac{\omega_o}{Q}}{s^2 + s\frac{\omega_o}{Q} + \omega_o{}^2}$$

(2) $$Q = \omega_o / \Delta\omega$$

Although representing the band-pass filter of interest using Laplace domain methods is easy, approaching the problem using a state space method will be much more illuminating. In state space, the band-pass filter can take limitless forms which all result in the same solution. A very common form for a state space model of a second order equation like the one shown in (1) is shown in (3), where the input vector of the band-pass filter is **x**(t), and the output of the band-pass filter is y(t). The form shown in (3) will be of particular use. The equations shown in (4) explicitly show the constants from (3). Bolded terms refer to vectors.[1]

(3) $$\begin{aligned} \dot{\mathbf{x}}(t) &= A\mathbf{x}(t) + bu(t) \\ y(t) &= c\mathbf{x}(t) + d \end{aligned}$$

(4)
$$\dot{\mathbf{x}}(t)=\begin{pmatrix} -\frac{\omega_o}{2Q} & -\omega_A \\ \omega_A & -\frac{\omega_o}{2Q} \end{pmatrix}\mathbf{x}(t)+\frac{\omega_o}{2Q}\begin{pmatrix} 1 \\ -1 \end{pmatrix}u(t);$$
$$y(t)=[(-\gamma+\lambda) \quad (-\gamma-\lambda)]\mathbf{x}(t)$$

(5)
$$\gamma=\frac{1}{2Q}; \qquad \lambda=\sqrt{1-\gamma^2}; \qquad \omega_A=\lambda\omega_o$$

In the state matrix A above, the elements a_{11} and a_{22} are directly related to the sharpness of the filter, whereas the elements a_{12} and a_{21} are directly related to the center frequency of the filter. One of the most advantageous results of being able to represent the system as a system of state equations is that it allows the manipulation of those equations using state transformation matrices. By carefully choosing a time-varying state transformation matrix M(t), the band-pass filter and first local oscillator stages can be combined. The transformation matrix is given in (5), where ω_M is the modulation frequency of the oscillator.[2]

(6)
$$M(t)=\begin{pmatrix} \cos(\omega_M t) & \sin(\omega_M t) \\ -\sin(\omega_M t) & \cos(\omega_M t) \end{pmatrix}$$

Because the transformation matrix is time-dependent, the mathematical operations demonstrated in the following equations in (7) must apply, so that the form in (8) is obtained.

(7)
$$\dot{M}(t)=\begin{pmatrix} -\omega_M\sin(\omega_M t) & \omega_M\cos(\omega_M t) \\ -\omega_M\cos(\omega_M t) & -\omega_M\sin(\omega_M t) \end{pmatrix}$$
$$M(t)^{-1}=\frac{1}{\sin^2(\omega_M t)+\cos^2(\omega_M t)}\begin{pmatrix} \cos(\omega_M t) & -\sin(\omega_M t) \\ \sin(\omega_M t) & \cos(\omega_M t) \end{pmatrix}$$

(8)
$$\dot{\mathbf{x}}'(t)=M(t)^{-1}\left(M(t)A+\dot{M}(t)\right)\mathbf{x}'(\mathbf{t})+bu$$

After applying the transformation, the state matrix "A" experiences a notable transformation in (9). The only change to the state matrix is that the center frequency of the band-pass filter has changed.[1]

(9)
$$A' = \begin{pmatrix} -\frac{\omega_o}{2Q} & \omega_M - \omega_A \\ \omega_A - \omega_M & -\frac{\omega_o}{2Q} \end{pmatrix}$$

Seeing as the transformation matrix is time-varying already, we can use it to perform gain-control operations on the band-pass filter. The transformation matrix M(t) will be modified to be that which is shown in (10). The M(t) matrix inverse and derivative are shown in (11).[1]

(10)
$$M(t) = f(t) * \begin{pmatrix} \cos(\omega_M t) & \sin(\omega_M t) \\ -\sin(\omega_M t) & \cos(\omega_M t) \end{pmatrix}$$

(11)
$$\dot{M}(t) = \dot{f}(t) * \begin{pmatrix} \cos(\omega_M t) & \sin(\omega_M t) \\ -\sin(\omega_M t) & \cos(\omega_M t) \end{pmatrix} + f(t) \begin{pmatrix} -\omega_M \sin(\omega_M t) & \omega_M \cos(\omega_M t) \\ -\omega_M \cos(\omega_M t) & -\omega_M \sin(\omega_M t) \end{pmatrix}$$
$$M(t)^{-1} = \frac{1}{f(t)} \begin{pmatrix} \cos(\omega_M t) & -\sin(\omega_M t) \\ \sin(\omega_M t) & \cos(\omega_M t) \end{pmatrix}$$

As is seen in (12) the modified state matrix now as another term. The term which has been added will be referred to as the "fdot/f term" (the derivative of f(t) divided by f(t)) for the remainder of this document.

(12)
$$A' = \begin{pmatrix} -\frac{\omega_o}{2Q} + \frac{\dot{f}(t)}{f(t)} & \omega_M - \omega_A \\ \omega_A - \omega_M & -\frac{\omega_o}{2Q} + \frac{\dot{f}(t)}{f(t)} \end{pmatrix}$$

The (df(t)/dt)/f(t) term above can be chosen so that the term f(t) is the same as the amplitude of the AM signal being received by into the AM radio receiver system. If this

choice of f(t) in the state matrix is chosen, then it will be shown that this gain control method can greatly improve the frequency response of the filter, even when the Q-factor is very high. Ideally, even if the 3dB bandwidth of the filter is narrower than the signal bandwidth, the desired signal f(t) can be fully reconstructed as though it had not been attenuated at all.

C. Realization of "fdot/f" Term

The time domain solution's convenience for solving this problem is quite evident, as it allows the designer to add the fdot/f term to the filter system and get favorable results. However, all of the calculations that have been performed so far have proceeded under the assumption that the function f(t) is known for all time. Divining f(t) requires more mathematical rigor and a few approximations. *Figure 3* contains a simplified block diagram of the feedback system.

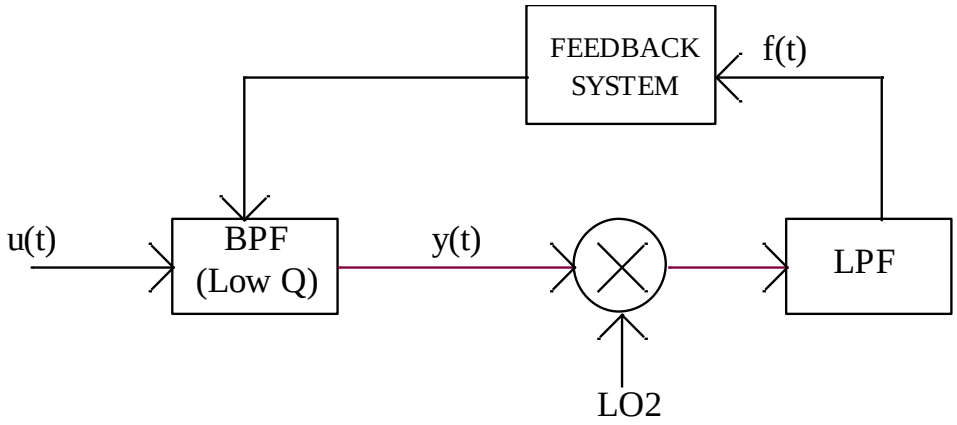

Figure 3: Feedback System Control Loop Block Diagram

The output of the band-pass filter is shifted down to the baseband by the second local oscillator in the AM radio receiver system in *Figure 3* above. After low-pass filtering the output of the local oscillator, the function f(t) is produced as the input to the feedback system. The feedback system produces the fdot/f term in the state matrix of the band-pass filter.

In order to make the feedback system easily realizable with real circuit components, a simple circuit is proposed in order to produce the fdot/f term. If the output of the low-pass filter in *Figure 3* above is fed into a first order low-pass filter with a particular cutoff frequency ω_k, then it would be easy to use just this filter to also effectively produce a high pass filter. The high pass filter can be produced by subtracting the output of the low-pass filter from the input of the low-pass filter. Let the low-pass filter's output be called y1(t), and the high pass output y2(t). Since the input to both filters is f(t), in the Laplace domain, we can see Y1(s) and Y2(s) as they are shown in (13) and (14) below.

(13) $$Y_1(s) = \frac{\omega_k}{s + \omega_k} F(s)$$

(14) $$Y_2(s) = \frac{s}{s + \omega_k} F(s)$$

If it is assumed that ω_k is very large compared to the frequency of f(t), then the transfer function from Equation (14) above can be approximated by the equation shown in (15).

(15) $$Y_2(s) \cong \frac{s}{\omega_k} F(s)$$

The Laplace operator "s" can be seen as the operator d/dt in the time domain. If y2(t) is divided by y1(t), the result shown in (16) would be obtained using the approximation given in (15). Multiplying by ω_k gives the result in (17).

(16) $$\frac{y_2(t)}{y_1(t)} \cong \frac{\dot{f}(t)}{\omega_k * f(t)}$$

(17) $$\omega_k \frac{y_2(t)}{y_1(t)} \cong \frac{\dot{f}(t)}{f(t)}$$

The mathematics process for deriving the fdot/f term of the feedback system can be represented using the block diagram in *Figure 4* below. The electronic components necessary for the construction of the feedback system are simple: one low-pass filter, one subtracting circuit, one divider, and one amplifier circuit.

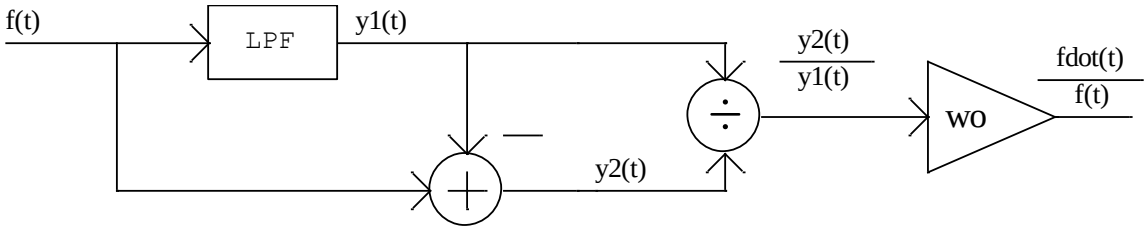

Figure 4: Block Diagram for Feedback System

The effective transfer function of the system shown in *Figure 4* can be found in Equation (18).

(18) $$H_{\text{Feedback System}}(s) = \frac{s\omega_k}{s + \omega_k}$$

D. Time-Varying Nature of Feedback and Radio Receiver Systems

One of the major assumptions of the feedback system is that the output of the AM radio receiver system is the desired signal f(t). This is permissible only because the Q-factor of the band-pass filter is small enough that the entire f(t) signal is not attenuated. The sharpness of the band-pass filter does not stay this broad indefinitely. As the feedback system begins to properly feed the gain-control term into the state matrix of the band-pass filter, the system will reach equilibrium operation. Prior to this equilibrium, the feedback system's output will not be incorporated into the band-pass filter. When the equilibrium operation is reached, feedback can begin, and a slow ramp-up of the Q-factor can begin.

The time-varying nature of the entire system allows for the manipulation of the components within the band-pass filter. The Q-factor can be easily modified over time

with modification of simple circuit components. A slow increase in the sharpness of the filter ideally will not affect the equilibrium operation of the entire system, and allow the feedback system to properly aid in the reconstruction of the side bands, even if the filter is narrower than the input bandwidth. The following sections will attempt to show through simulation that this time-varying strategy may yield desirable results.

II. Numerical Representation of System's Outputs

A. Numerical Approximation of Band-Pass Filter Output

All plots and computations were performed using MATLAB version 2010a. The system of differential equations represented by the state space equations for the band-pass filter must be properly discretized to yield the most accurate results. While many first-order discretization methods may work for the differential equations, some may require that the sampling frequency be very high. To effectively develop a numerical solution to the system of differential equations, a 2nd Order Gear continuous to discrete ("s" to "z") mapping was utilized. Considering second order mappings, no other mapping is more stable than the second order Gear.[3] The mapping shown in (19) demonstrates the mapping. The same mapping is applied to all other continuous to discrete mappings in the course of the simulations.

(19) $$s = \frac{1}{T}\left(\frac{1}{2}z^{-2} - 2z^{-1} + \frac{3}{2}\right)$$

Although the band-pass filter can be seen in the time domain as shown in (20), the Laplace representation in (21) lends itself to being discretized using the mapping described in (19).

(20) $$\dot{\mathbf{x}}(t) = A*\mathbf{x}(t) + \mathbf{b}*u(t)$$

(21) $$s\mathbf{X}(\mathbf{s}) = A*\mathbf{X}(s) + \mathbf{b}*U(s)$$

The equation shown in (22) is the mapping of (21) to the z-domain, and can be rearranged and manipulated to reach the final discrete-time system. In discrete time, the solution can be viewed as the equation seen in (23).

(22) $$\frac{1}{T}\left(\frac{1}{2}z^{-2} - 2z^{-1} + \frac{3}{2}\right)\mathbf{X}(z) = A\mathbf{X}(z) + \mathbf{b}U(z)$$

(23) $$\mathbf{x}(n) = \left(\frac{3}{2}I - TA\right)^{-1}\left(2\mathbf{x}(n-1) - \frac{1}{2}\mathbf{x}(n-2) + T\mathbf{b}u(n)\right)$$

B. Numerical Approximation of the Final Low-Pass Filter Output

The low pass filter which feeds into the feedback system must also be low pass filtered to remove the high frequency components resultant from the frequency shift down to the baseband. The 2nd order Gear mapping will be utilized for this discrete transformation as well. The low pass filter consists of a fourth order Butterworth filter, where f_{01} = 20kHz; Q_1 = 0.541; f_{02} = 20kHz; Q_2 = 1.306.[4] Developing the filter requires two separate, second-order Butterworth filters, which each have a transfer function designated by (24) where "m" in the subscripts is replaced with the number related to the stage for each filter.

(24) $$H(s) = \frac{\omega_{0m}{}^2}{s^2 + \frac{\omega_{0m}}{Q_m}s + \omega_{0m}{}^2}$$

The Butterworth filters will be discretized using the same continuous-to-discrete mapping as shown in (19). The transfer function in the z-domain is given by (25). The system solved and rearranged so that the output can be easily approximated in discrete time is shown in (26).

$$(25)\qquad H(z)=\frac{{\omega_{0m}}^2}{(\frac{1}{T}\left(\frac{1}{2}z^{-2}-2z^{-1}+\frac{3}{2}\right))^2+\frac{\omega_{0m}}{Q_m}(\frac{1}{T}(\frac{1}{2}z^{-2}-2z^{-1}+\frac{3}{2}))+{\omega_{0m}}^2}$$

$$(26)\qquad y(n+1)=\frac{1}{(\frac{1}{T^2}+\frac{\omega_{0m}}{TQ_m}+{\omega_{0m}}^2)}\left(\frac{2}{T^2}+\frac{\omega_{0m}}{TQ_m}\right)y(n)-\frac{1}{T^2}y(n-1)+{\omega_{0m}}^2u(n+1))$$

The output of the discrete time Butterworth filter will be followed by another just like it, except with the index "m" replaced with "2". The "y" in the equation above is related to the output of the filter, while "u" relates to the input.

C. Numerical Approximation of the Feedback System Output

The feedback system possesses the over-all Laplace domain transfer function found in (18). The transfer function will also be discretized for the purposes of simulation using the 2nd order Gear shown in (19). After using this mapping, the z-domain transfer function becomes that which is found in (27).

$$(27)\qquad H(z)=\frac{(\frac{1}{T}(\frac{1}{2}z^{-2}-2z^{-1}+\frac{3}{2}))\omega_k}{\frac{1}{T}(\frac{1}{2}z^{-2}-2z^{-1}+\frac{3}{2})+\omega_k}$$

After performing the necessary algebraic rearrangement for the relation of the output of the feedback system to the input of the feedback system in discrete time, the result is the equation in (28). The term "y" refers to the output of the feedback system, while the term "u" refers to the input of the feedback system.

$$(28)\qquad y(n+1)=\left(\frac{1}{\frac{3}{2}+T\omega_k}\right)(2y(n)-\frac{1}{2}y(n-1)+\frac{\omega_k}{2}u(n-1)-2u(n)+\frac{3\omega_k}{2}u(n+1))$$

III. Simulation Methods and Preliminary Testing

A. Simulation Method

All discrete Fourier transform (DFT) plots are subjected to the Blackman windowing method to improve their clarity.[5] For the sake of this experimentation, the carrier frequency will be set to 100kHz. All simulations are run to an end time of 0.1 seconds with a sampling frequency of 10MHz. In all DFT plots, the DFT is performed on the final quarter of the samples, so as not to include any transients in the output.

In the following sections, the feedback control system will be exercised with different inputs as well as different levels of ideality. The same plots and information will be taken from each case, and compared in a table in section VIII, part A. For each case, a time domain plot of the radio receiver system output will be given, and plotted in comparison to the desired signal f(t). Other important plots that will be included will be two plots of the magnitude spectrum for each case, one where the frequency range of the x-axis of the plot varies between 89kHz and 112kHz, and one where the frequency range is much narrower to give a better view of the attenuation of the sidebands. The narrower view will range between 3.2kHz and 3.16MHz. For the first few tests, the DFT plot of the input will also be included, but as this will become redundant in later tests, the figures associated with those plots will be referenced in those cases.

In order to exercise each system, the sideband function f(t) will be a sinusoidal signal with a positive DC offset. The signals which will represent f(t) in each test of the radio receiver system will be the ones found in (29) and (30). In addition to exercising each system with two different inputs, each system will also encounter each input with added white noise in the input

(29) $$f(t) = 2 + \sin(2\pi * 1000t)$$

(30) $$f(t) = 2 + \sin(2\pi * 2000t)$$

In addition to two different types of inputs, the same tests will be conducted with and without the addition of "white noise" which is produced using the "randn" function in MATLAB. This function produces a string of random numbers, and in the case for this project, the standard deviation will be set to 0.1, while the mean will remain at zero. How the system handles noise will be a key metric in deciding the quality of the solution.

In the first set of tests, the fdot/f term was analytically calculated and a vector for its values was generated in MATLAB. This process will be repeated for each test pertaining to ideal gain control. In these cases, it is assumed that the desired signal f(t) can be perfectly predicted, and the fdot/f term can be perfectly generated. In amplitude modulated signals, it is necessary to have a DC component be a part of the function f(t) so that the function does not have a zero crossings. The transformation matrix mentioned in (12) earlier requires that f(t) have an inverse for all time, so the DC component is indeed helpful.

Unlike the first set of tests, which contain many idealized elements, the second set of tests will implement a parallel network of two band-pass filters, one with a relatively small Q-factor (Q=1) and another with a large Q-factor (Q=50). The output of the band-pass filter with the smaller Q-factor will be used as the input to a copy of the feedback system mentioned earlier, and the output of that feedback system will be fed into the state equations of the band-pass filter with the higher Q-factor. This way, the fdot/f term is being produced by the actual feedback system, it just isn't implemented in a full feedback loop yet. A diagram of this system is given in *Figure 5*. The local oscillators and the low pass filter blocks are the same for both parts of the parallel system.

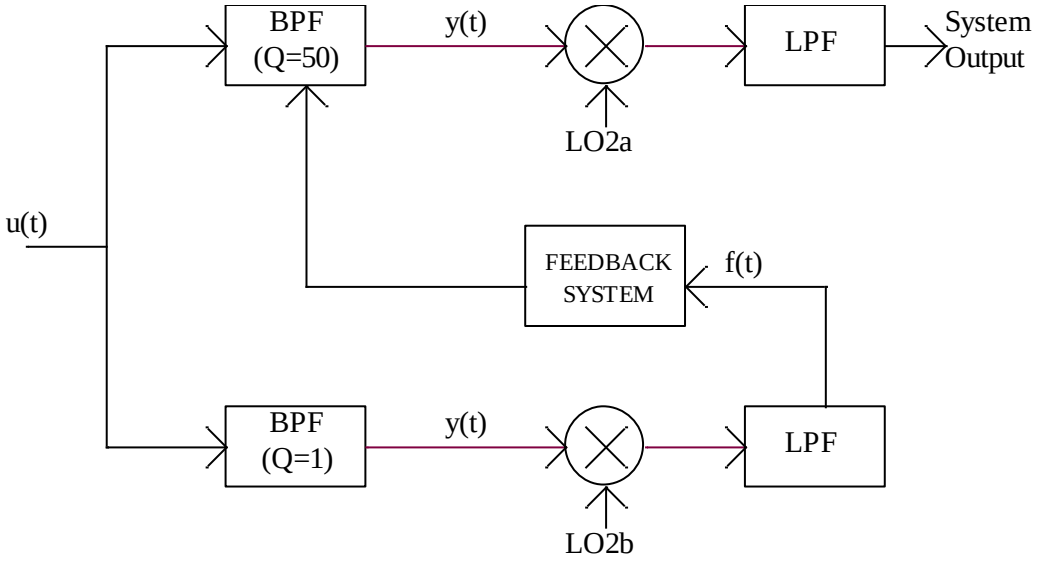

Figure 5: Parallel System For Use in Simulation

Finally, the system to be tested will be the entire feedback loop system, as indicated in *Figure 3*. For the feedback system, the first 0.01 seconds (of the total run time of 0.1 seconds) will be used a "preamble time", where the output of the feedback system won't be input into the core band-pass filter. The feedback system will be allowed to reach equilibrium while the Q-factor is still small enough not to attenuate the sidebands. After this preamble time, the feedback will be switched on. The Q-factor will then ramp up over a period of 0.39 seconds with the goal of minimizing attenuation of the sidebands. After the Q-factor has finished ramping up, the system will remain at its new equilibrium operation.

B. Exercising the Feedback System in Open Loop

Before moving on to testing the system with the use of the feedback system, it is important to verify that the feedback system does in fact output the fdot/f term accurately. Setting the sharpness of the band-pass filter such that it does not attenuate the sidebands, we can rearrange the AM radio receiver system block diagram to see how well the

feedback system performs. In this test, the AM radio receiver system is changed to be the block diagram shown below in *Figure 6*.

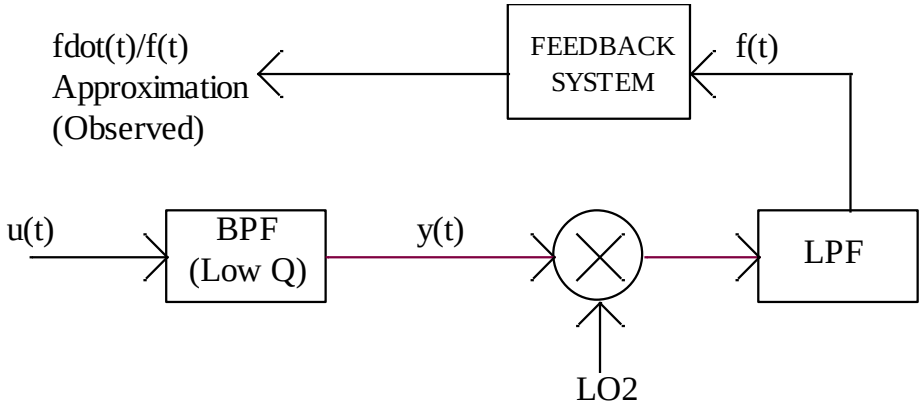

Figure 6: Open Loop Feedback System Block Diagram

In this test, the Feedback system accepts the un-attenuated signal u(t) which is down-converted to become an approximation of f(t). This f(t) is then processed by the feedback system. The output of the feedback system ("fdot(t)/f(t) Approximation Observed" in *Figure 6* is shown in *Figure 7* compared to the plot of the actual fdot/f term. In this case, f(t) is the same as the function shown in (29).

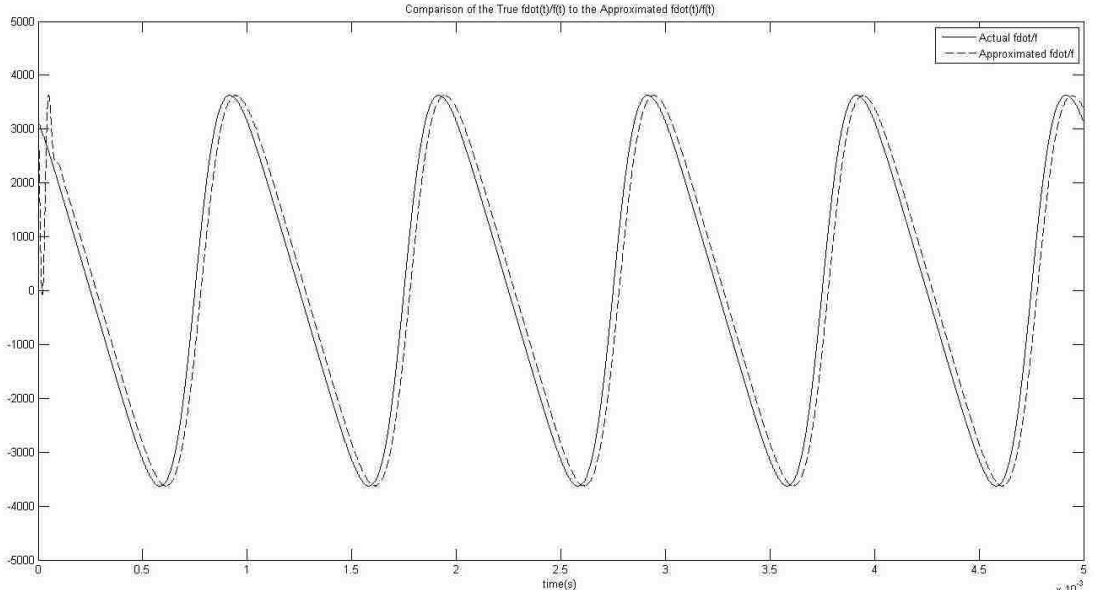

Figure 7: Approximate and True fdot/f Plots For 1kHz Sidebands

In open loop, the amplitude error on the approximated fdot/f term is only 0.08%, while the phase difference is only 10.40 degrees. The phase difference is largely a result of the low-pass filters acting in the system.

The open loop system will now be subjected to an input which carries a sideband signal f(t) with the same properties as (30). The resultant approximate fdot/f term compared to the actual fdot/f term is plotted in *Figure 8*.

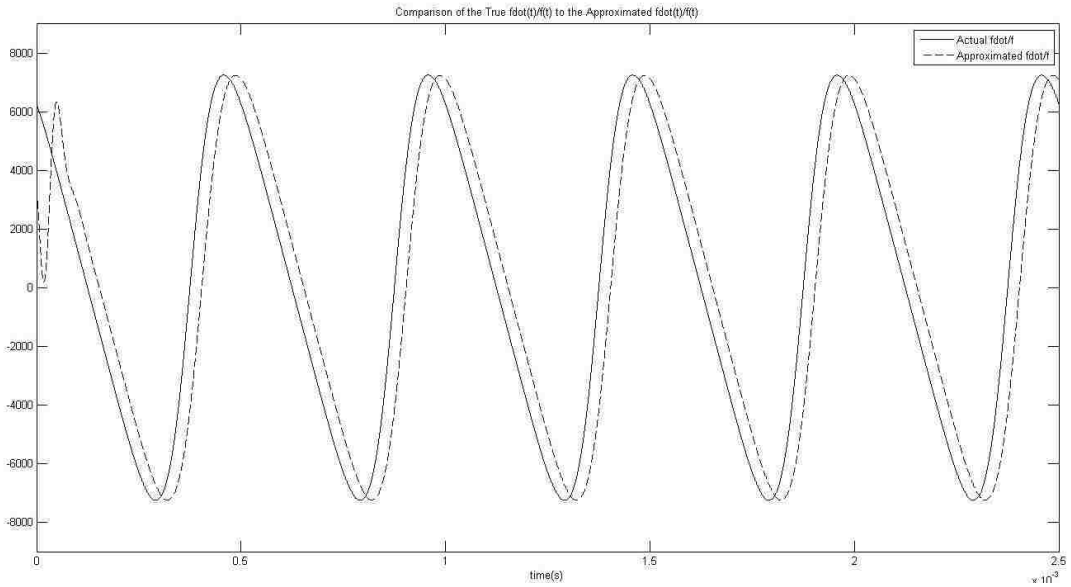

Figure 8: Approximate and True fdot/f Plots For 1kHz Sidebands

This test is encouraging in terms of amplitude error as, but the phase difference is significantly larger than before. This can be attributed to the high order low pass filter which feeds into the feedback system. The amplitude error is 0.096%, and the phase difference is 20.8 degrees. Clearly, as the frequency of the input to the system grows, so does the phase shift. In the tests that will be performed, it will become clear that phase shift plays an important role in the success of the feedback system.

IV. Results When Applying Idealized Fdot/f term

A. Application of Ideal Gain Control with 1kHz Sidebands

In the ideal gain control experiments, the system is simulated as though the function f(t) and the fdot/f term of the state matrix can be perfectly predicted and used in the system. These tests are to show that if the feedback system is working properly, the sidebands can be reconstructed successfully. In this test, the Q-factor of the filter is 50. Seeing as the center frequency of the filter is 100kHz, this means that the 3dB bandwidth of the filter is 2kHz. As a result the sidebands would each be attenuated by about 3dB, as they are each 1kHz away from the center of the band-pass filter.

The first plot for the first experiment is the DFT plot of the input signal to the band-pass filter. As is evident in *Figure 9*, the input to the band-pass filter is centered at the frequency shifted carrier frequency.

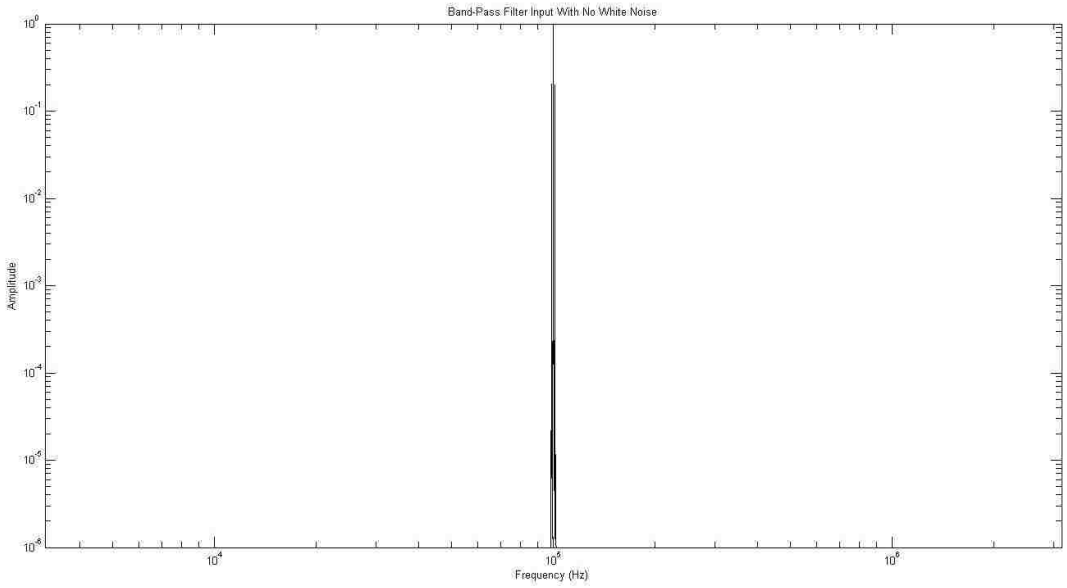

Figure 9: Ideal Noiseless BPF Input DFT 1kHz Sideband

The next result is the input signal over a smaller frequency range so as to observe the sidebands of the signal. Although the approximations made in the plotting of these magnitude spectra alter the expected peak values of the impulses, an accurate comparison can be drawn between the magnitude of the input sidebands and the magnitude of the output sidebands. See *Figure 10* for a closer look at the magnitude spectra of the input to

the band-pass filter. In *Figure 10*, the sidebands have been normalized along with the carrier signal by using the Blackman windowing method. The impulses associated with the signal f(t) attached to the carrier signal possess magnitudes of 0.2052 and 0.1988 for the left band and the right bands respectively. As the sampling frequency approaches infinity, the sidebands could be seen to approach 0.25 in magnitude each.

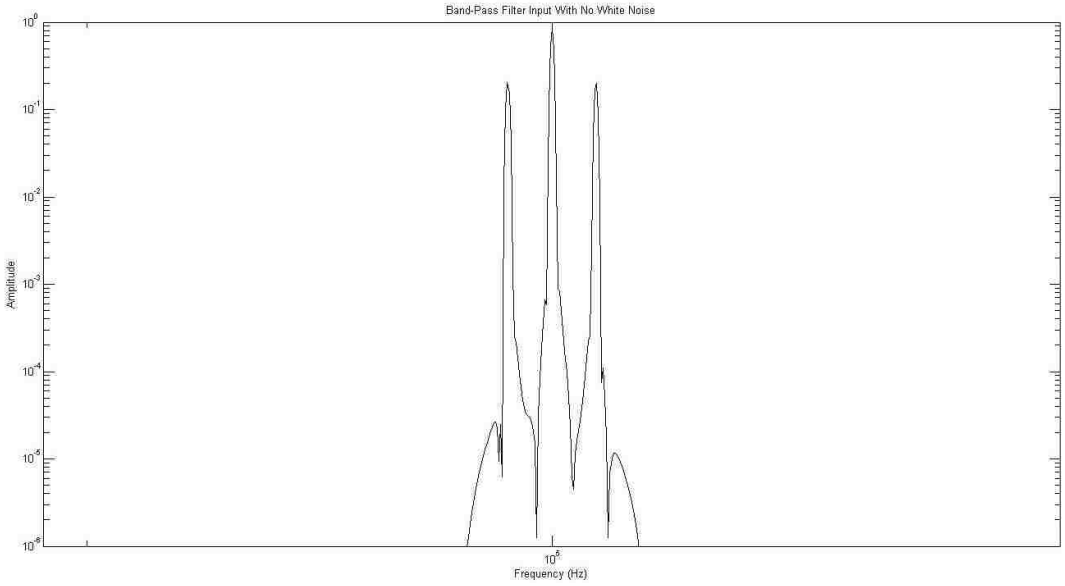

Figure 10: Ideal Noiseless BPF Input DFT 1kHz Sideband

Because no noise has been added to the input of the system, the plot in *Figure 10* may appear redundant. However, the plot gives a clear indication that there is noise floor added by the system in action. The sideband peaks occur at 101kHz and 99kHz as was expected.

After zooming in for a closer look at the DFT plot of the band-pass filter output, the output appears to be quite promising in terms of attenuation. When the ideal gain control is applied to the band-pass filter state matrix, the output of the band-pass filter experiences almost no attenuation. In the output, the left and right sideband magnitudes are 0.2019 and 0.1956, respectively. Compared to the plot of the magnitude spectra of the input to the band-pass filter, the attenuation is only 1.7% for each part of the signal.

If the ideal gain control signal had not been applied to this system, the attenuation would have been 3dB, or about 29.3%. See *Figure 11* for the plot in question.

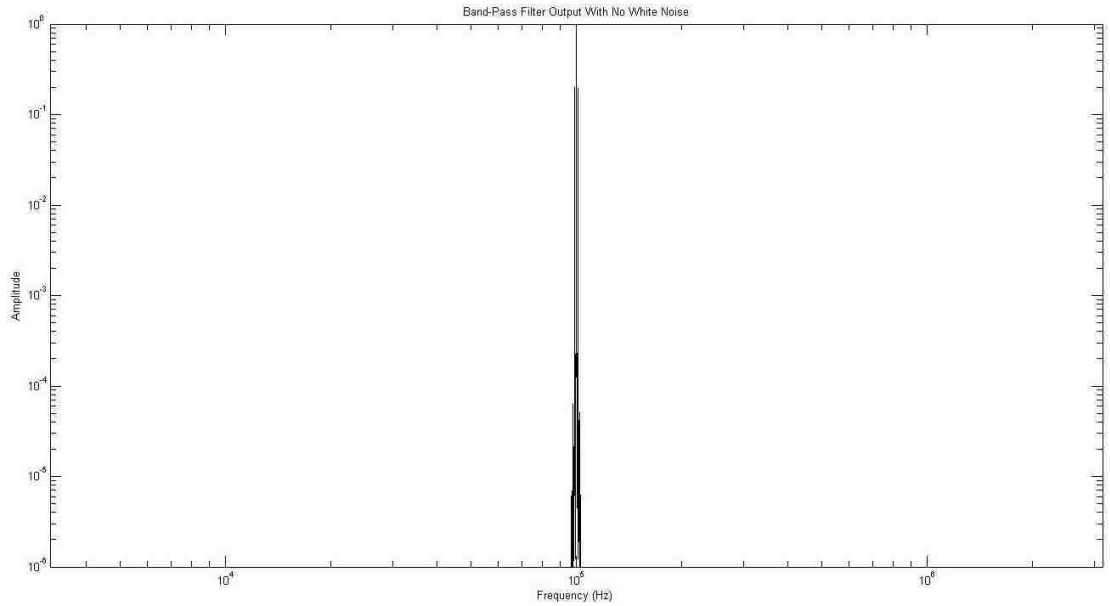

Figure 11: Ideal Noiseless BPF Output DFT 1kHz Sideband

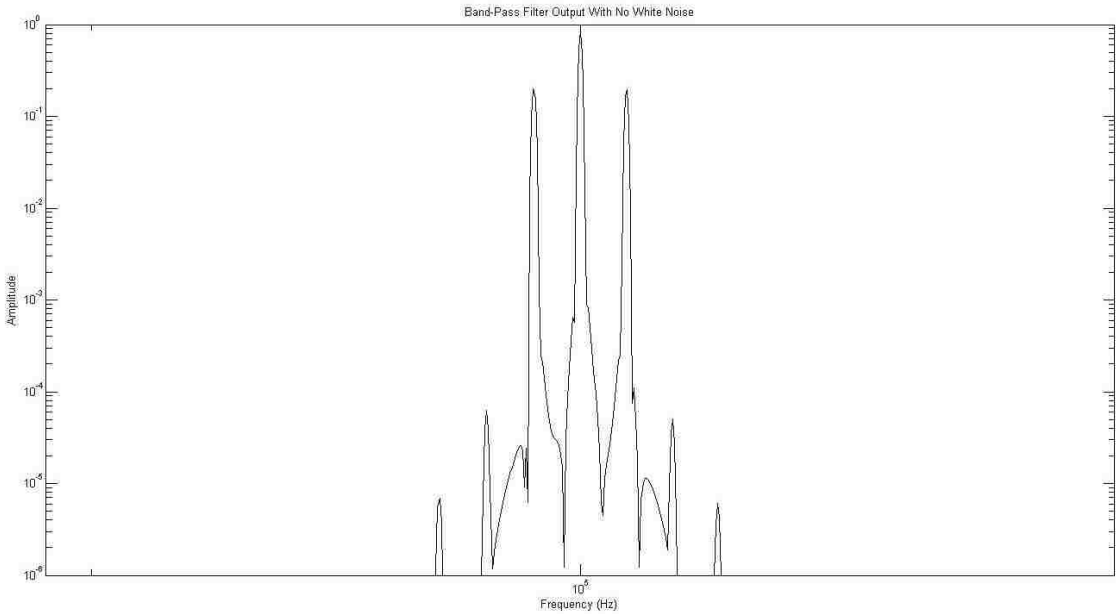

Figure 12: Ideal Noiseless BPF Output DFT Zoomed In 1kHz Sideband

Harmonic distortion can be seen in the plot given in *Figure 12*. This is due to imperfections in the fdot/f term. Discretizing the idealized fdot/f term appears to add enough error that harmonic distortion is noticeable on a log scale. However, the

distortion is over three orders of magnitude smaller than the desired signal, so the distortion doesn't pose any threat to the signal.

The last plot from the first test (*Figure13*) is a comparison between the desired signal f(t) and the final output of the AM radio receiver system. The amplitude of the output signal has only a1.8% attenuation, just what was shown in the DFT plot for the sidebands.

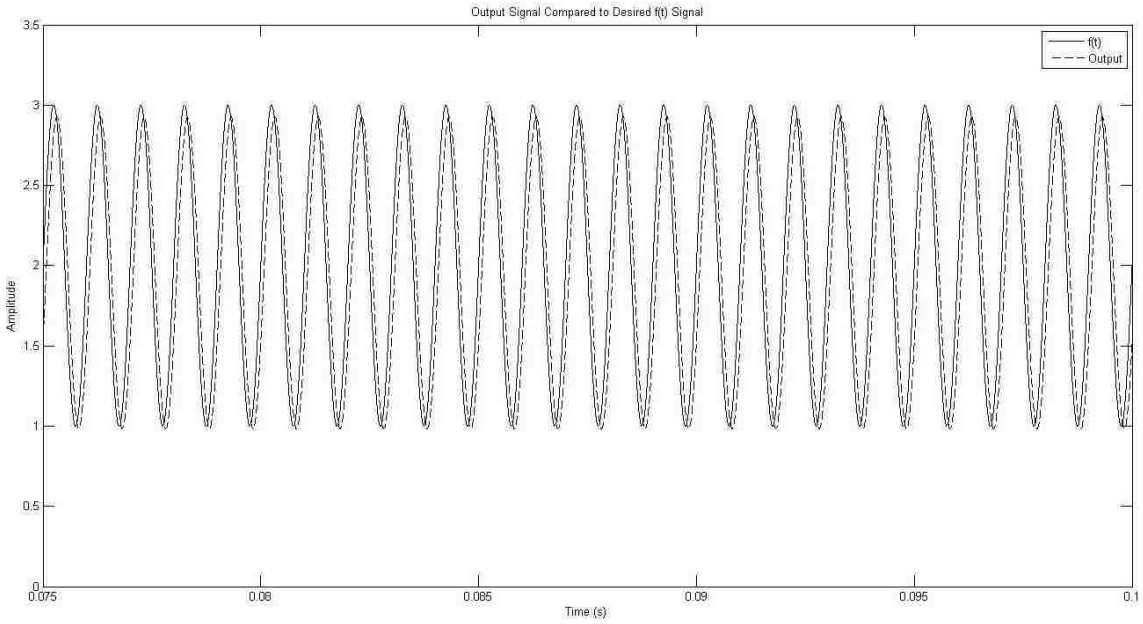

Figure 13: Ideal Noiseless System Output and f(t) Comparison 1kHz Sideband

B. Application of Ideal Gain Control with 1kHz Sidebands and White Noise

While the totally ideal system seemed to deal fairly well with reconstructing the sidebands, adding noise can allow for the observation of manipulation of noise between the sidebands and the carrier frequency. *Figure 14* shows the input to the band-filter with white noise added.

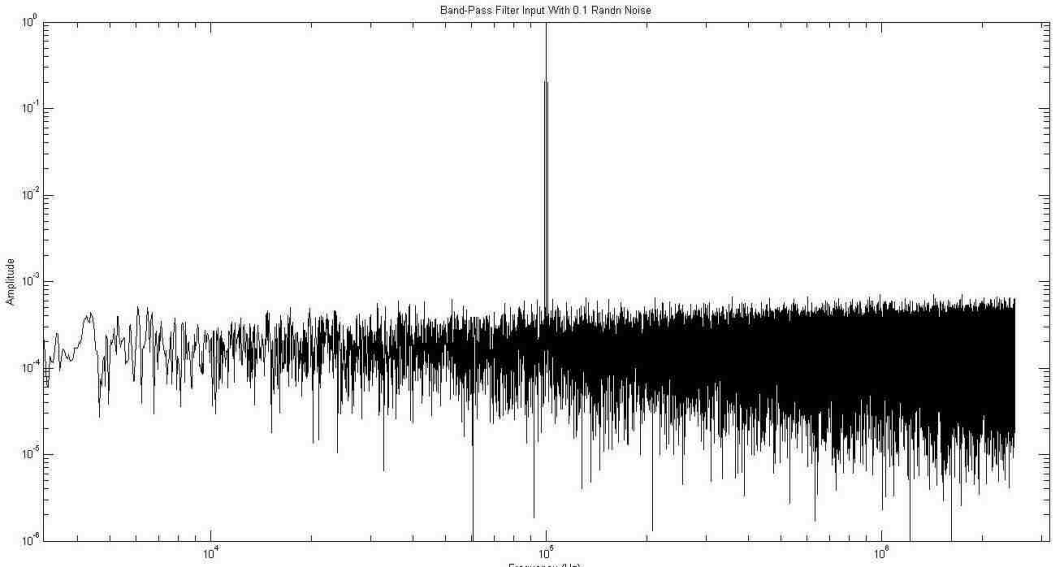

Figure 14: Ideal Noisy BPF Input DFT 1kHz Sideband

The left and right sidebands in the magnitude spectrum shown in *Figure 15* are 0.2051 and 0.1987, respectively. These impulses now have a noise floor around them which should be attenuated by the band-pass filter. *Figure 15* is simply a close-up view of the plot shown in *Figure 14*, this time with the x-axis (frequency) shown from $10^{4.95}$ to $10^{5.05}$ Hz.

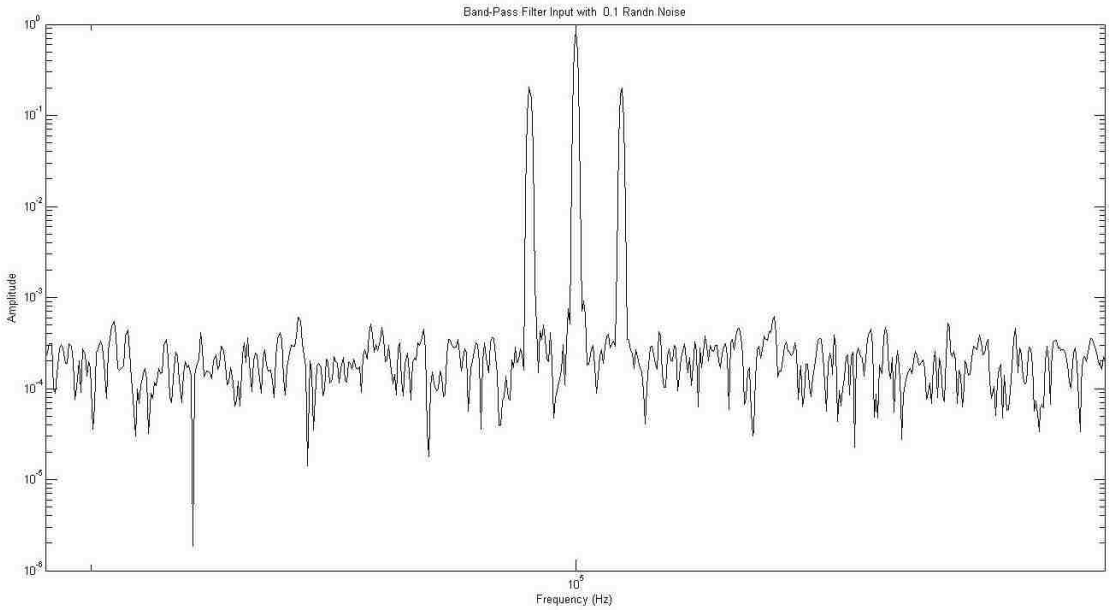

Figure 15: Ideal Noisy BPF Input DFT 1kHz Sideband Zoomed In

It is clear from *Figure 16* that the band-pass filter is performing its basic function properly – attenuating noise at approximately 20dB per decade outside of the 3dB cutoff bandwidth. A closer look at the frequency spectrum of the output of the band-pass filter will be more revealing.

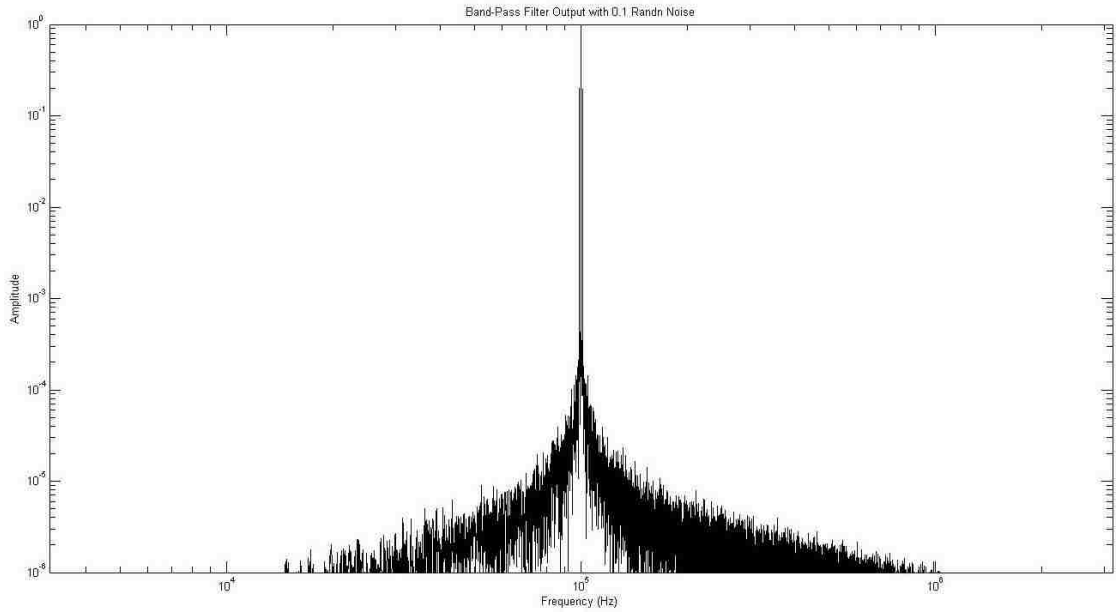

Figure 16: Ideal Noisy BPF Output DFT 1kHz Sideband

The sidebands have been successfully reconstructed to the same degree of accuracy as when no noise was present in the system. The left and right sidebands are 0.2019, and 0.1955, respectively, and have experienced attenuation of 1.6% each. On another positive note, the noise between the sidebands and the central impulse has also been attenuated. The noise closest to the sidebands was attenuated by 14.7%.

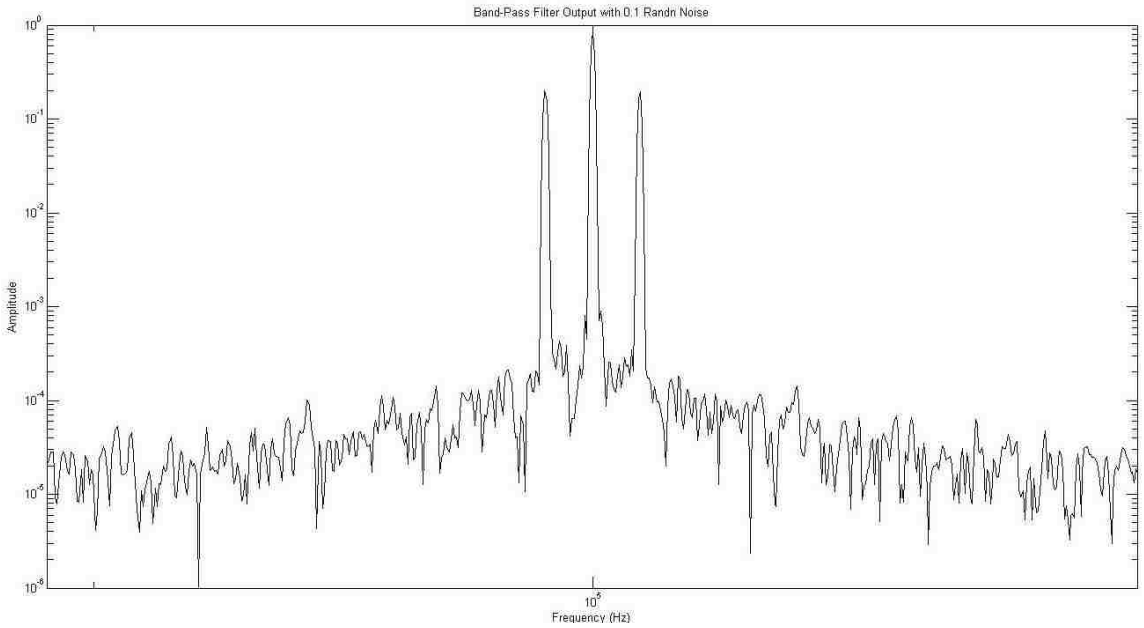

Figure 17: Ideal Noisy BPF Output DFT 1kHz Sideband Zoomed In

C. Application of Ideal Gain Control with 2kHz Sidebands

The next step to exercise the system is to apply an input to the band-pass filter with a wider gap between the sidebands and the carrier signal. The amount of reconstruction needed for the sidebands in this case is greater than for the 1kHz input case, as the sidebands experience more attenuation due to the core band-pass filter with the same Q-factor of 50. The expected attenuation of the sidebands without the feedback is approximately 5dB, or about 44%.

Figure 18 makes it clear that there is no noise floor present in the input of the system. No harmonic distortion, or other imperfections are apparent. *Figure 18* will act as a reference for future plots for the non-ideal system with a 2kHz input.

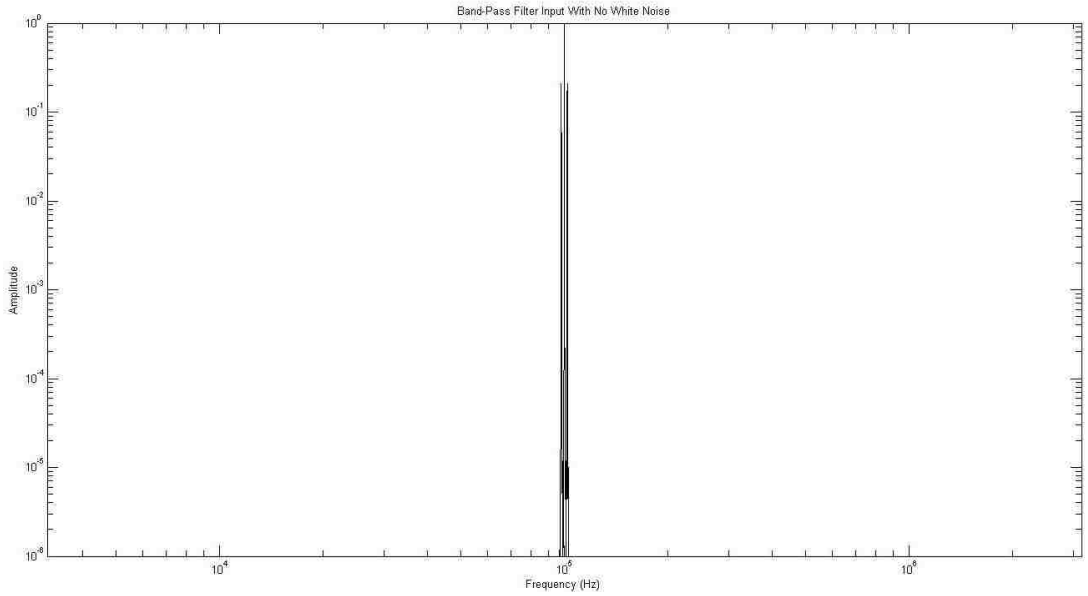

Figure 18: Ideal Noiseless BPF Input DFT 2kHz Sideband

A closer look at the input magnitude spectrum using *Figure 19* reveals that the sidebands are indeed almost exactly the same size as they were in the case where the sideband function f(t) contained a 1kHz sine wave. This time, the bands are now 2kHz away from the carrier frequency impulse. The heights of the left and right sidebands in this case are 0.2102 and 0.2084.

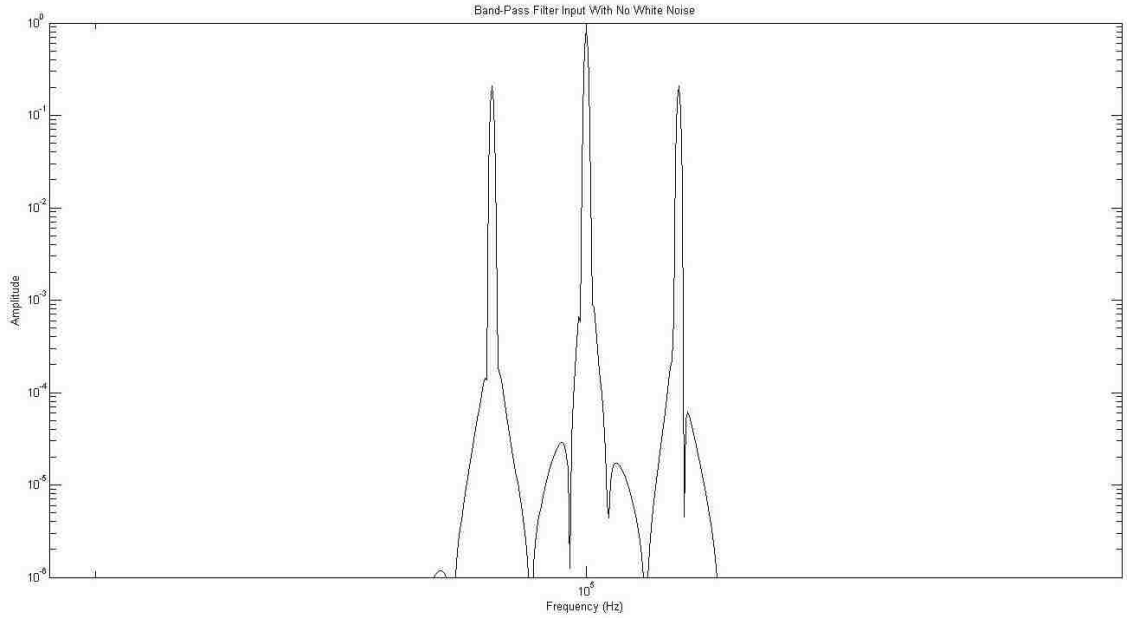

Figure 19: Ideal Noiseless BPF Input DFT 2kHz Sideband Zoomed In

The plot in *Figure 20* is of the magnitude spectrum of the output of the band-pass filter with the 2kHz sine wave sidebands. It is clear from the picture that some harmonic distortion is present, but no other major noise issues have arisen.

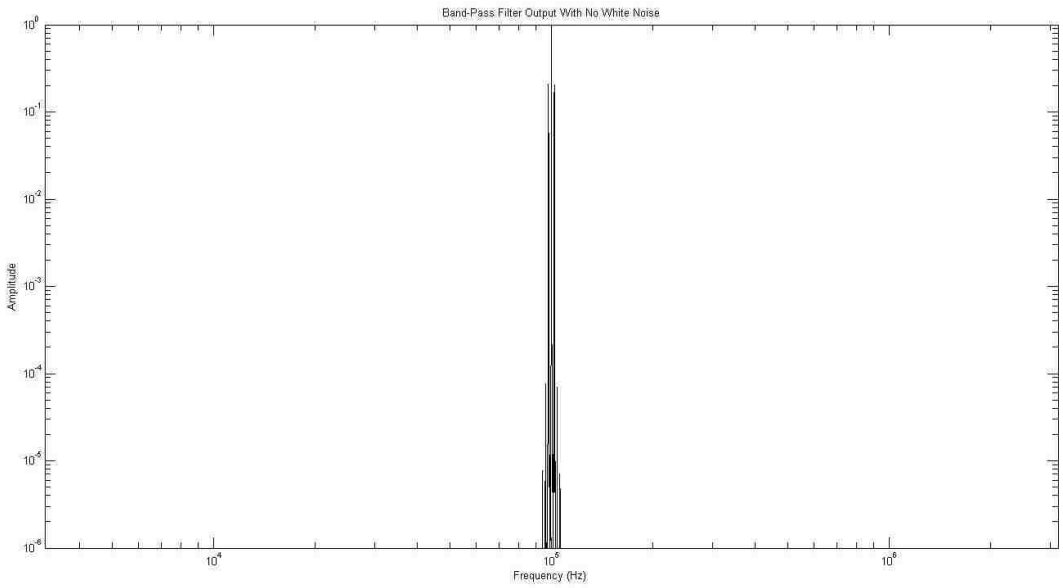

Figure 20: Ideal Noiseless BPF Output DFT 2kHz Sideband

Harmonic distortion similar to that observed in the noiseless case for the 1kHz sideband signal is present in the plot of the output of the band-pass filter given the current input. The plot of this case is shown in *Figure 21*. The left and right sidebands are of heights 0.2064 and 0.2048, respectively. This indicates that the attenuation of the sidebands is only 1.8%, which is highly favorable. The harmonic distortion observed in the output of the band-pass filter almost a full five orders of magnitude smaller than the sidebands.

In accordance with the attenuation of the sidebands, the output of the AM radio receiver system is only attenuated by approximately 1.8%. The plot of the output compared to the desired signal f(t) is plotted in *Figure 22*.

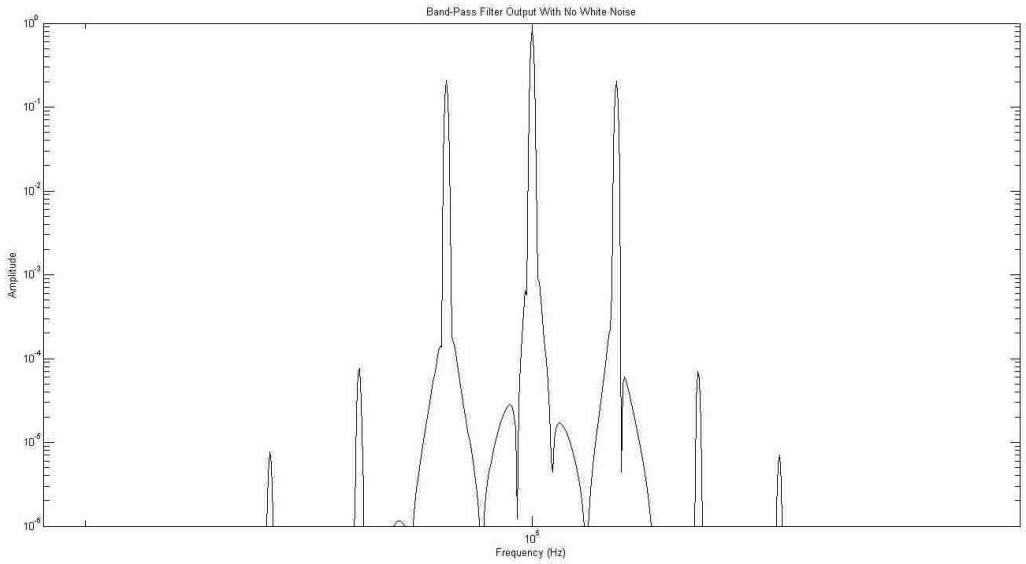

Figure 21: Ideal Noiseless BPF Output DFT 2kHz Sideband Zoomed In

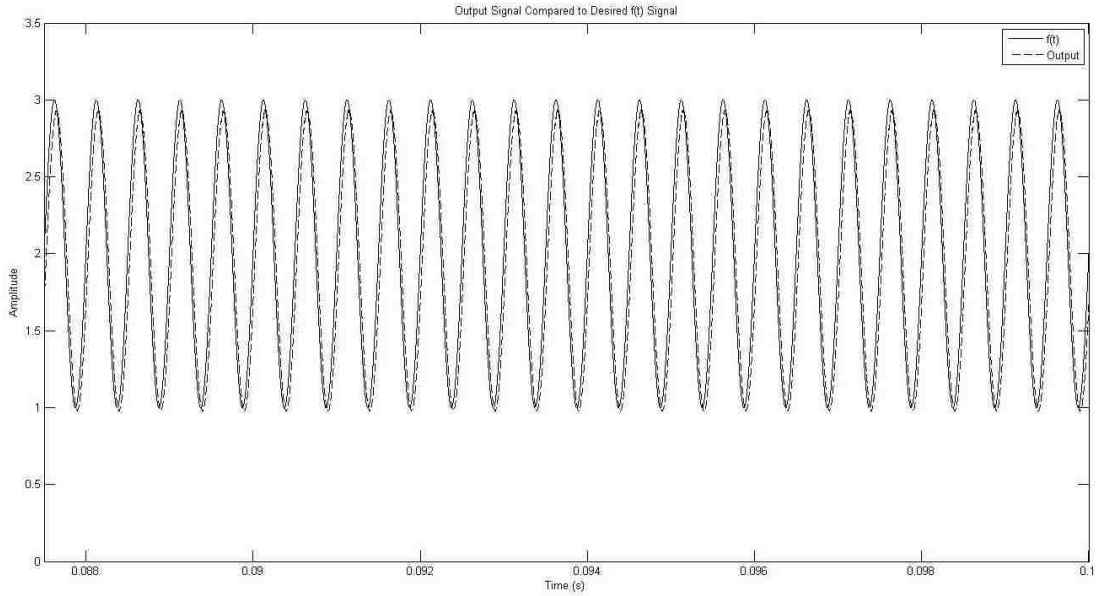

Figure 22: Ideal Noiseless System Output and f(t) Comparison 2kHz Sideband

D. Application of Ideal Gain Control with 2kHz Sidebands and White Noise

As before in the 1kHz case, the magnitude spectrum of the input to the band-pass filter has been plotted in *Figure 23.*

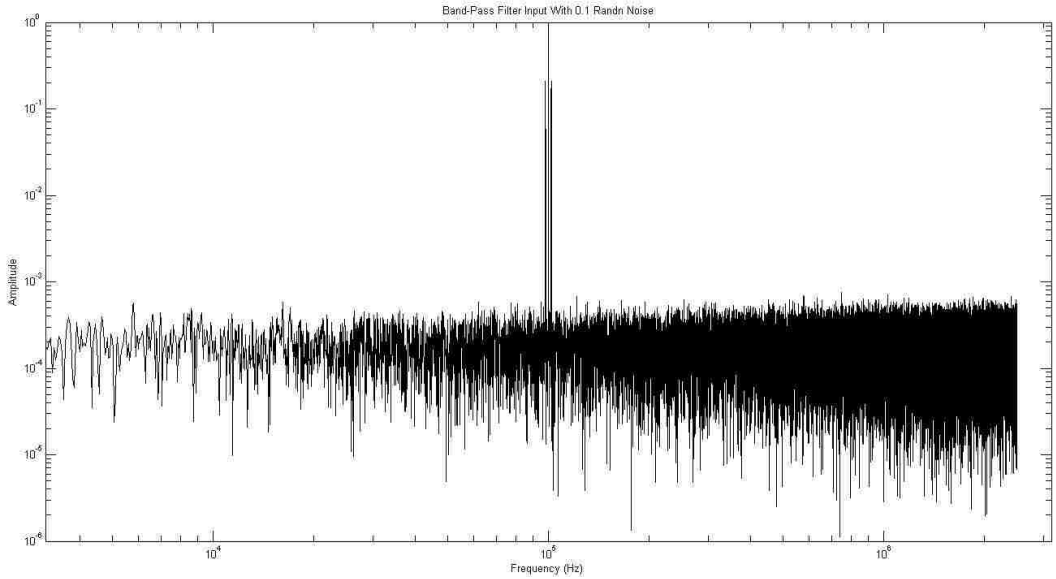

Figure 23: Ideal Noisy BPF Input DFT 2kHz Sideband

Taking a closer look at the input spectrum, the left and right sidebands are 0.2102 and 0.2082, respectively. A plot of the magnitude spectrum of the input over a smaller frequency range is shown in *Figure 24*.

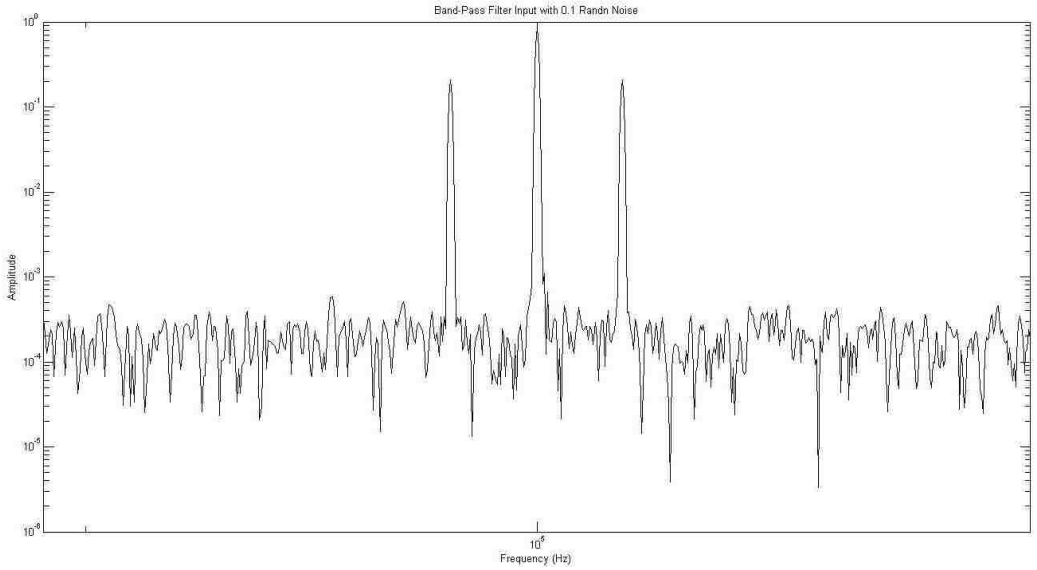

Figure 24: Ideal Noisy BPF Input DFT 2kHz Sideband Zoomed In

The band-pass filter is working properly on noise located outside its 3dB cutoff bandwidth as is clear from the DFT plot of the band-pass filter output in *Figure 25*.

On closer inspection of the output of the band-pass filter, the sidebands are once again only attenuated by 1.8% in *Figure 26*. Noise closest to the inner part of the sidebands has also been attenuated by 39.2%, which is greater than for the case where f(t) contained a 1kHz sinusoid and understandable given that the sidebands for the 2kHz case are further from the 3dB cutoff frequencies of the band-pass filter.

The time domain output of the radio receiver system also seems to be in good shape. The attenuation is only 1.8%. See *Figure 27* for a plot of the output compared to f(t) for this experiment. It appears that even with the addition of noise and sidebands that are 1kHz outside the 3dB cutoff bandwidth of the filter, this system is still able to reconstruct those sidebands.

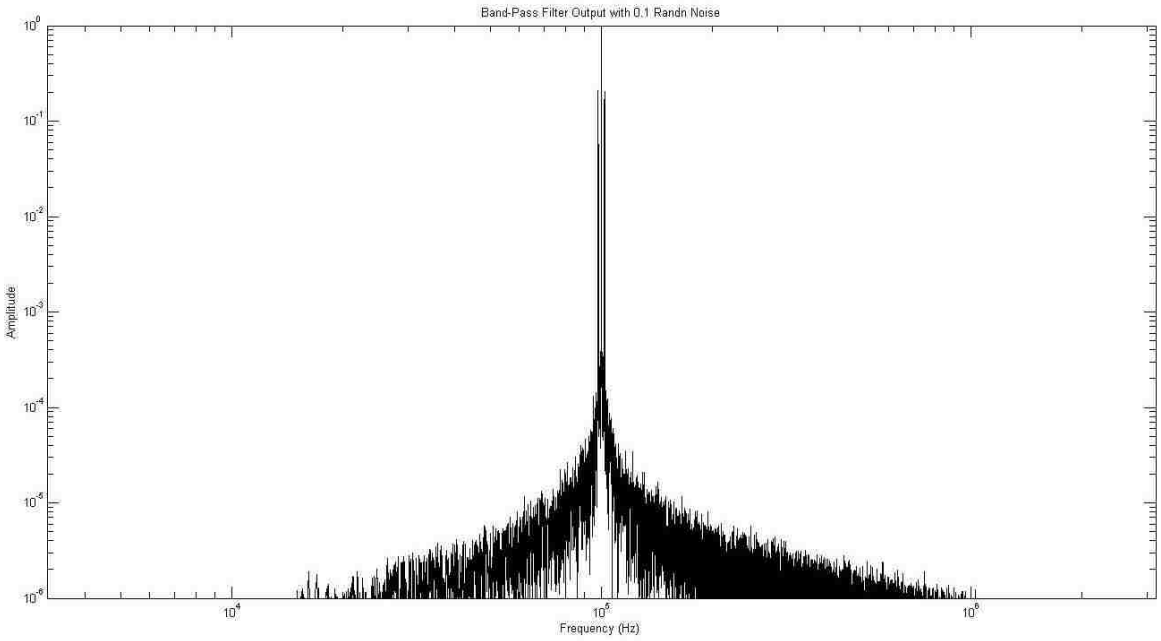

Figure 25: Ideal Noisy BPF Output DFT 2kHz Sideband

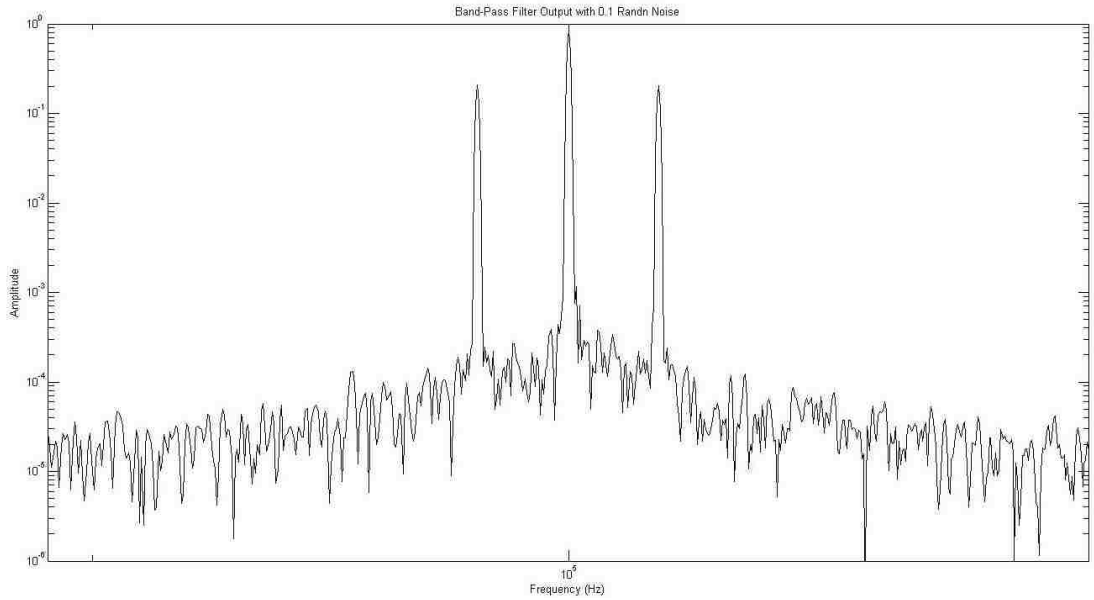

Figure 26: Ideal Noisy BPF Output DFT 2kHz Sideband Zoomed In

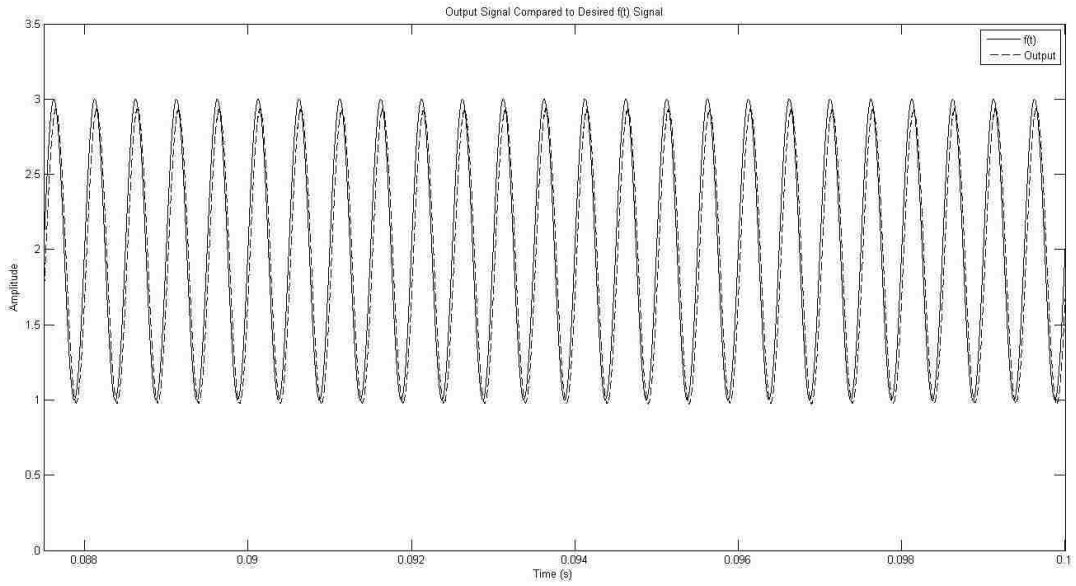

Figure 27: Ideal Noisy System Output and f(t) Comparison 2kHz Sideband

V. Results For Parallel System

A. Parallel System Tested with 1kHz Sidebands

While the idealized system ran smoothly, it was evident that any small errors in the fdot/f term that is fed back into the core filter will lead to significant harmonic distortion. In the case with 1kHz sidebands and no noise, the harmonic distortion was

made very clear. The first figure, *Figure 28* shows the spectrum of the output zoomed out, and it is already clear that harmonic distortion is present.

On closer inspection, the harmonic distortion is several orders of magnitude larger with the non-ideal fdot/f term being used. Although the left and right sidebands are not attenuated (they are 0.2216 and 0.2101, respectively), the largest peak in the harmonic distortion is 1.42% the size of the desired sidebands. See *Figure 29* for a zoomed in plot of the results from *Figure 28*. The harmonic distortion appears to be the result of slight phase shift in the fdot/f term.

As a result of the harmonic distortion, the output's quality appears to be quite poor. The magnitude of the output is not attenuated. In fact, it experiences a slight gain (about 5%) when compared to the desired signal f(t). However, the signal is not nearly as clean as it was when the ideal fdot/f term was being used. See *Figure 30* for a plot of the comparison for this case.

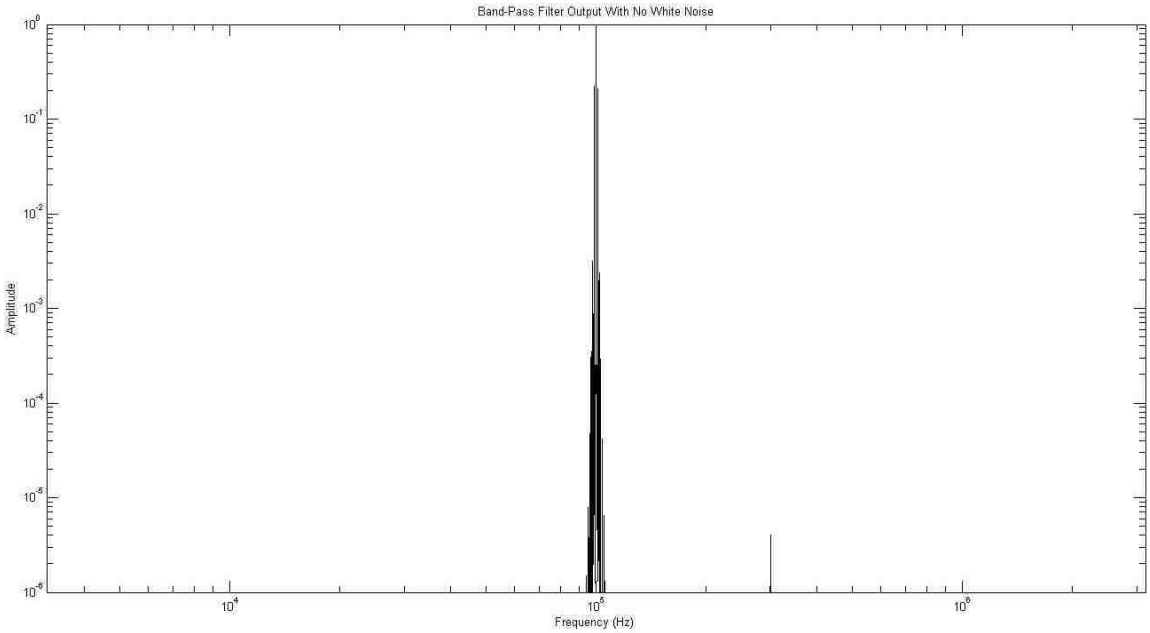

Figure 28: Parallel Noiseless BPF Output DFT 1kHz Sideband

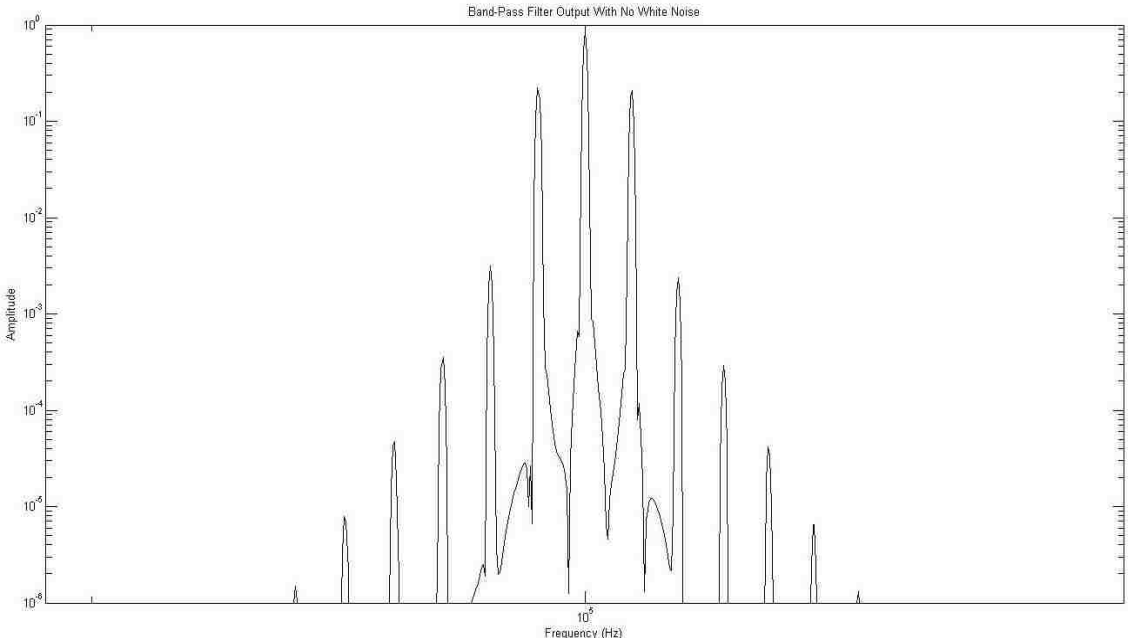

Figure 29: Parallel Noiseless BPF Output DFT 1kHz Sideband Zoomed In

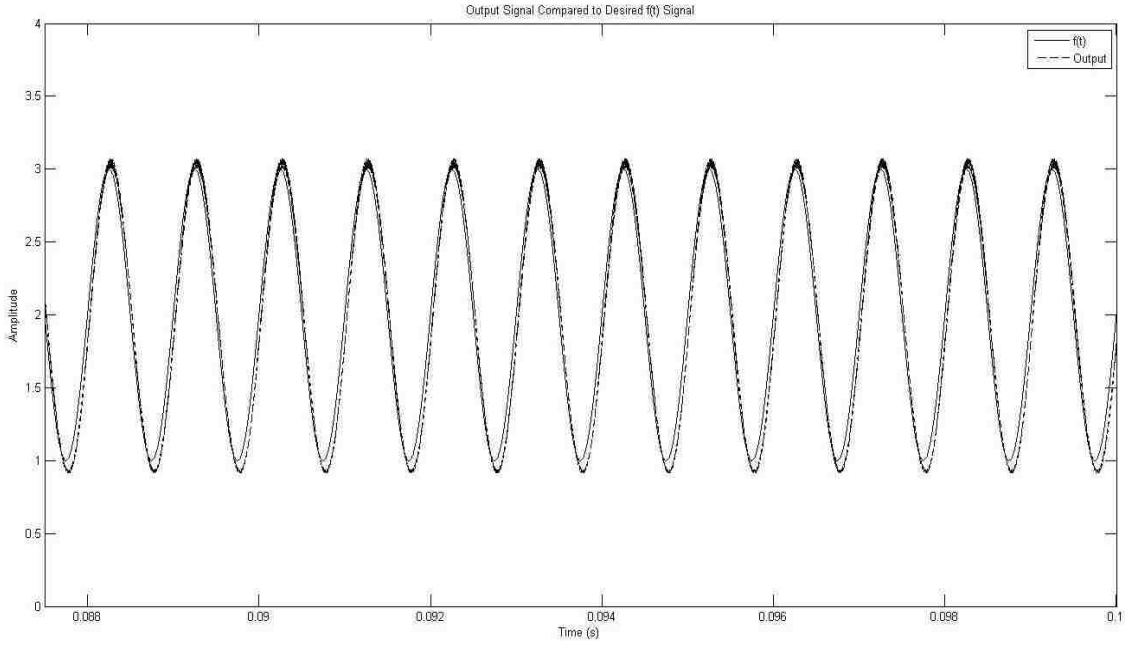

Figure 30: Parallel Noiseless System Output and f(t) Comparison 1kHz Sideband

B. Parallel System Tested with 1kHz Sidebands and Noise

The added white noise appears to do some of the work of burying the harmonic distortion. From a look at the plot over the larger frequency range in *Figure 31*, some of

the weaker harmonic distortion is no longer noticeable, as that distortion resided below the current noise floor.

The left and right sidebands in the DFT plot shown in *Figure 32* of the output have magnitude of 0.2215 and 0.2101, respectively. Just like in the noiseless case, the sidebands have a slight gain of about 5.4%. This gain and the harmonic distortion that's seen is a result of the imperfect fdot/f term.

The noise doesn't seem to have any major effects on the output of the radio receiver system. Although there is still some distortion, the output in this case is almost identical to the case where noise was not present in the input. The band-pass filter is still capable of rejecting the noise, not the distortion. See *Figure 33* for a plot of the output compared to f(t).

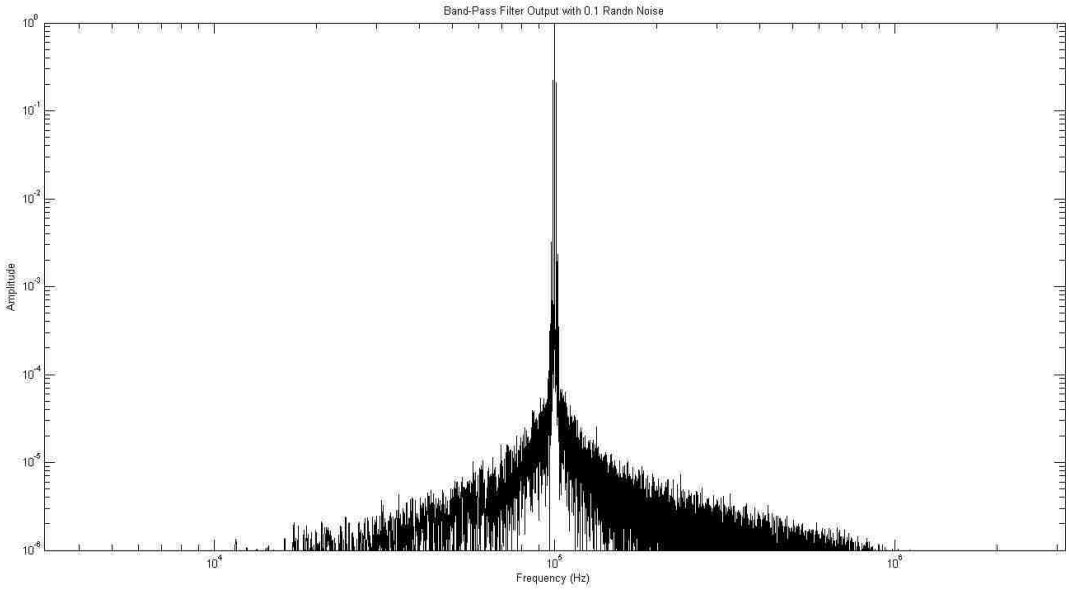

Figure 31: Parallel Noisy BPF Output DFT 1kHz Sideband

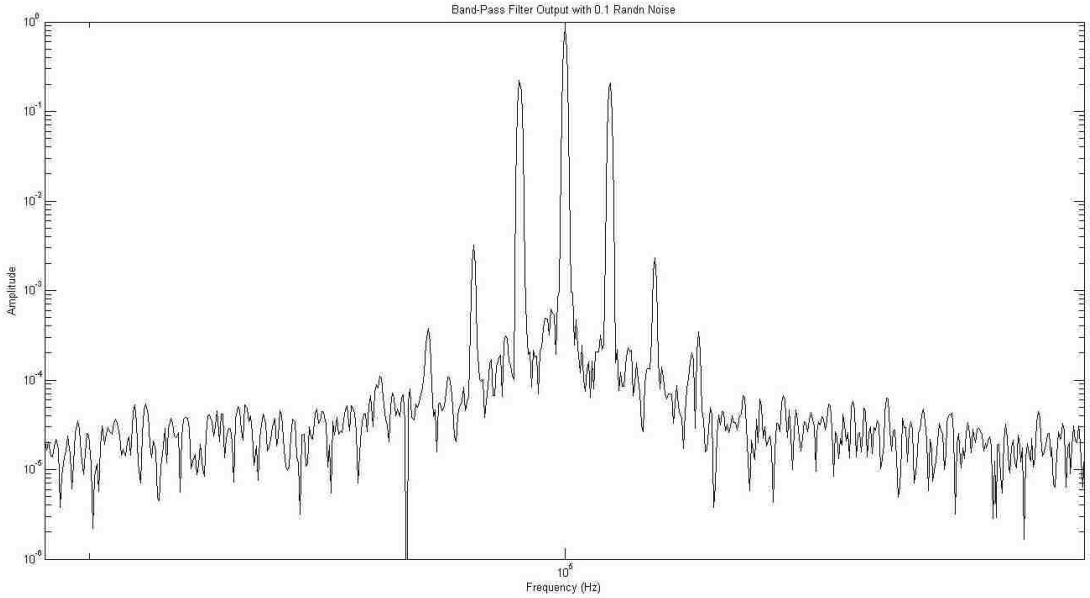

Figure 32: Parallel Noisy BPF Output DFT 1kHz Sideband Zoomed In

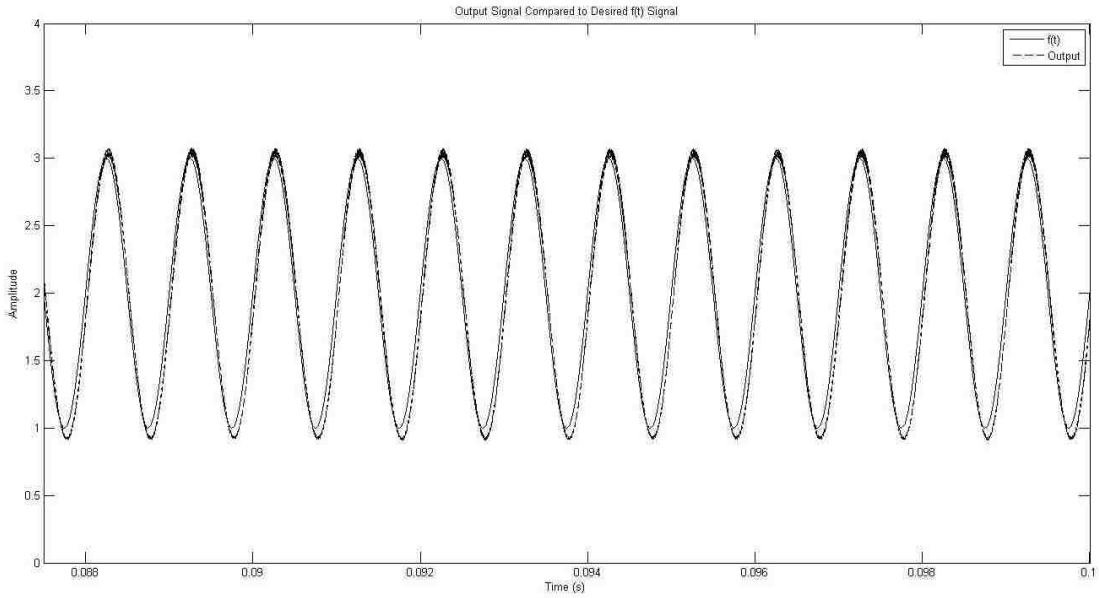

Figure 33: Parallel Noisy System Output and f(t) Comparison 1kHz Sideband

C. Parallel System Tested with 2kHz Sidebands

Without any white noise added to hide the harmonic distortion it begins to stand out as in *Figure 34* for the 2kHz sideband case. When zooming in on the DFT plot of the output of the band-pass filter, the left and right sidebands are found to be 0.2377 and 0.2292, respectively. Once again, a gain is found in the sidebands of about 9.5% in

Figure 35. The harmonic distortion is a harsh price to pay for this gain. The strongest harmonic distortion peak is at 3.85 thousandths. The gain of 9.5% can also be seen in the time domain plot of the output of the radio receiver system, which is compared to f(t) for this case in *Figure 36*.

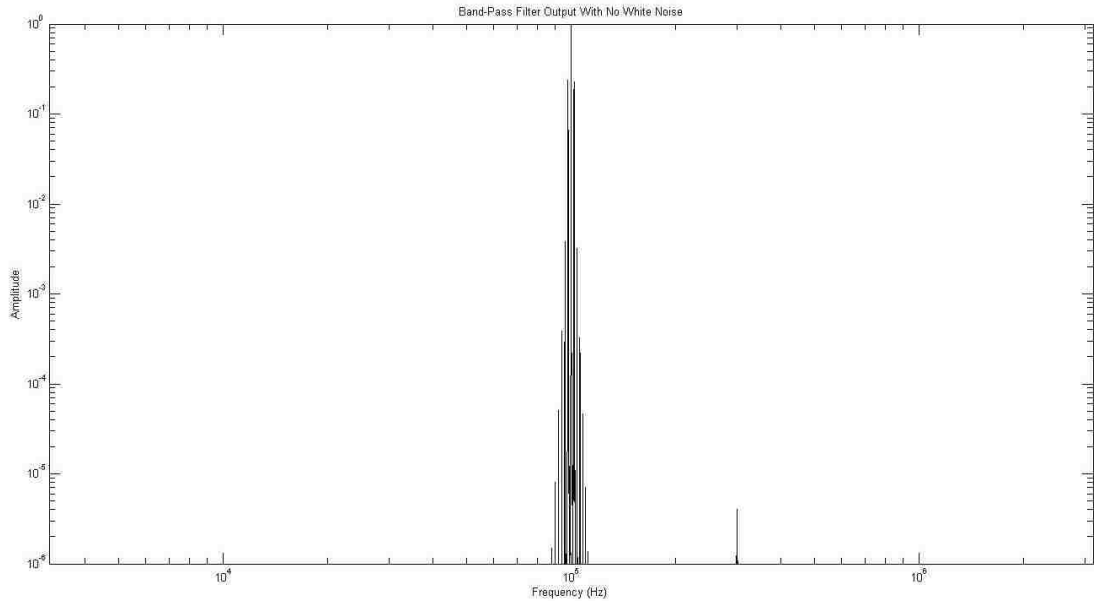

Figure 34: Parallel Noiseless BPF Output DFT 2kHz Sideband

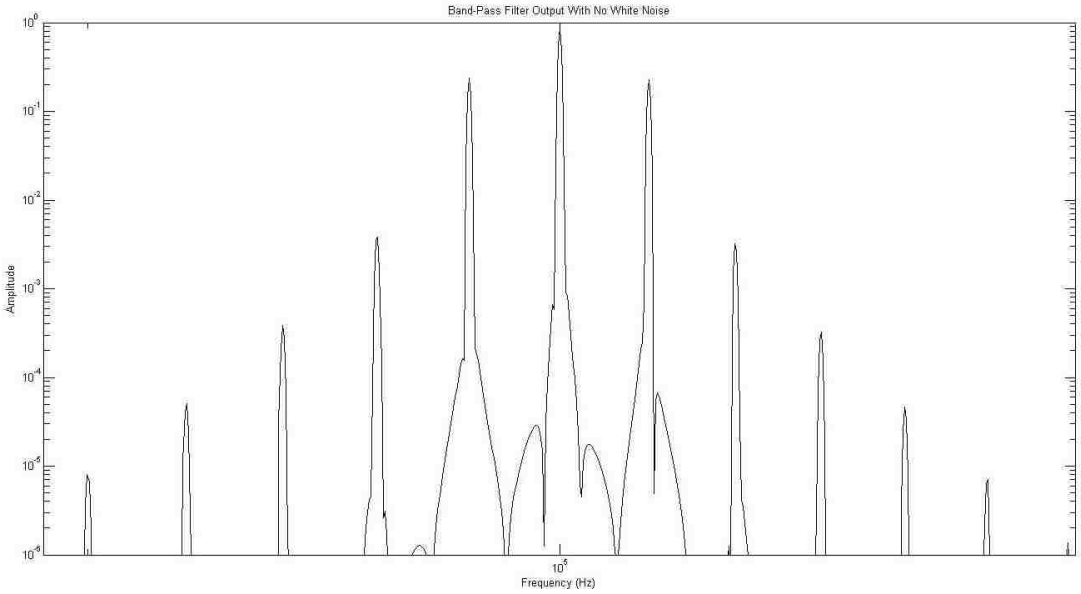

Figure 35: Parallel Noiseless BPF Output DFT 2kHz Sideband Zoomed In

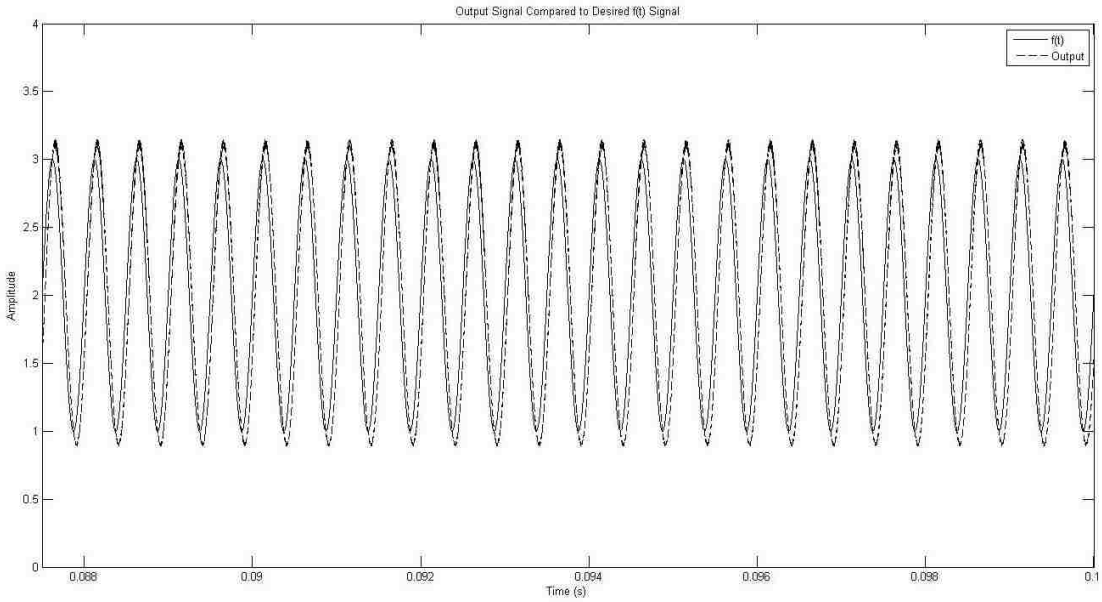

Figure 36: Parallel Noiseless System Output and f(t) Comparison 2kHz Sideband

D. Parallel System Tested with 2kHz Sidebands and Noise

For this test, the band-pass filter continues to perform its job in filtering out noise on a large scale. Some harmonic distortion is discernable from the plot in *Figure 39*. In the plot in *Figure 38*, the left and right sidebands possess heights of 0.2376, and 0.2293. This means that there is yet again a slight gain (about 12.9%) offered to the sidebands at the cost of additional harmonic distortion. Since the harmonic distortion appears to be caused by the additional phase added to the fdot/f term, the 2kHz sideband fdot/f term will pick up more phase while passing through the low-pass filter in the low Q-factor band-pass filter system. The peak of the tallest harmonic is read at 0.00378. The gain and distortion are evident in the time domain plot of the output shown in *Figure 39*.

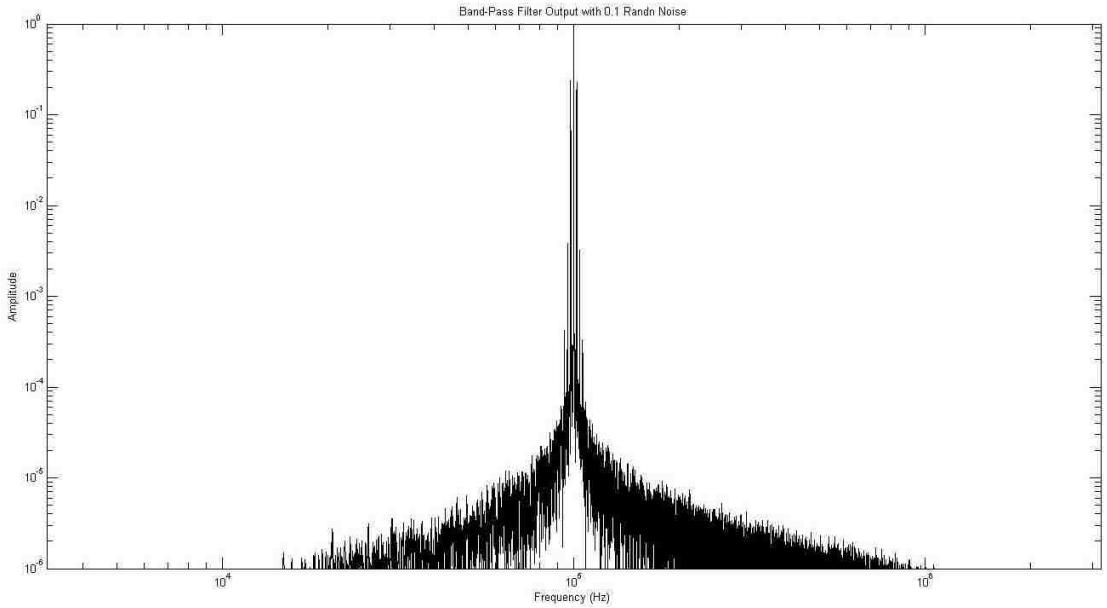

Figure 37: Parallel Noisy BPF Output DFT 2kHz Sideband

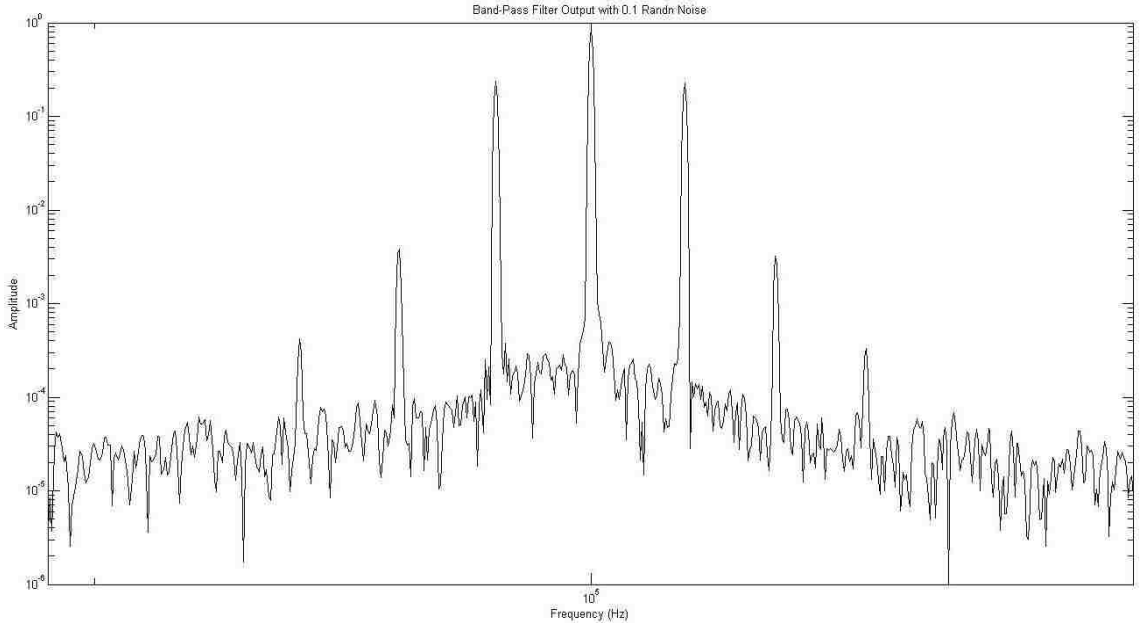

Figure 38: Parallel Noisy BPF Output DFT 2kHz Sideband Zoomed In

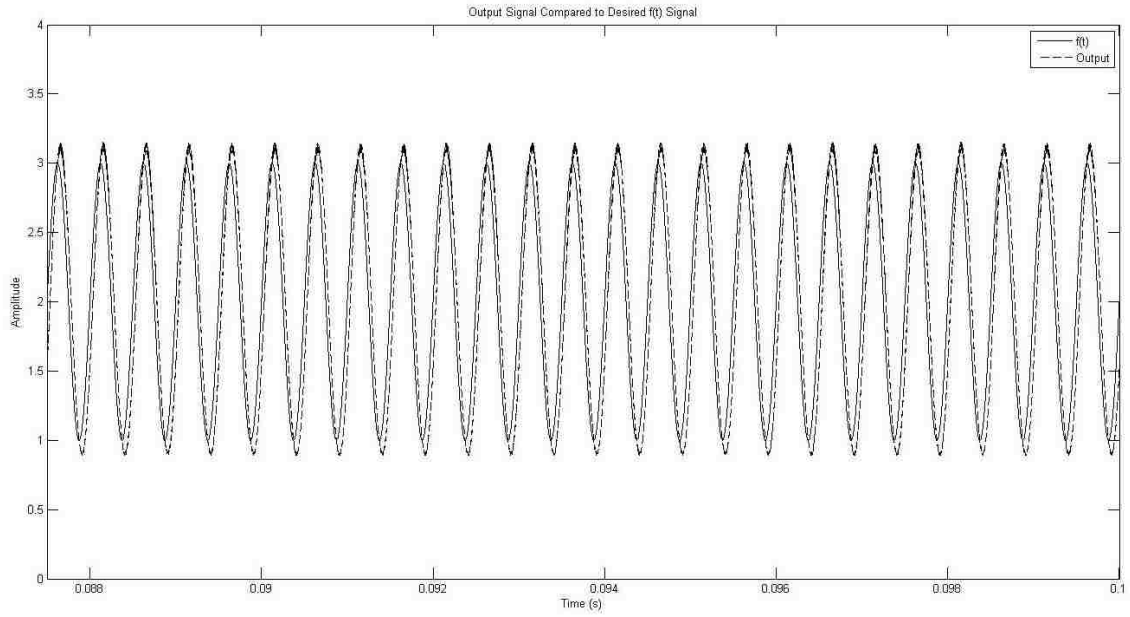

Figure 39: Parallel Noisy System Output and f(t) Comparison 2kHz Sideband

VI. Results For System With Feedback

A. Gain Control Plots Note

One important plot of note to include in the tests which involve the full feedback system is the plot of the approximated fdot/f term. The assumption has been made that the feedback system will find an equilibrium which will allow the sidebands to be constructed successfully. In the results which follow this section, the sidebands are successfully reconstructed, but a considerable amount of distortion is also present. Despite attempting many different Q-factor sloping rates, a true equilibrium could not be reached. Ramping up the Q-factor in any way resulted in distortion of the fdot/f term, and thus distortion of the output.

B. Full Feedback System Tested with 1kHz Sidebands

Compared to the input given in *Figure 9*, the DFT of the output of the band-pass filter looks quite messy. The harmonics are numerous and of rather large magnitude, and are even visible on a large scale plot like the one in *Figure 40*. Upon closer inspection of

the same plot in *Figure 41*, the number of noticeable harmonics is quite large. Though the gain for the sidebands is up to 11%, the harmonic distortion far outweighs these benefits, with the highest peaks of the distortion reaching 14.4% of the magnitude of the sidebands. The next peak from the harmonic distortion isn't much better at 8.2% of the magnitude of the sidebands.

Although much of the distortion is filtered out by the low-pass filter at the output of the radio receiver system, the output, which is plotted in *Figure 42* still ends up looking quite distorted. In *Figure 43* there is a plotted comparison between the idealized fdot/f term and the one that is approximated by this system. As is clear from the figure, the distortion of the fdot/f term begins when the Q-factor begins ramping. The amplitude of the approximated fdot/f term reaches a high at 5203, dwarfing the amplitude of the actual fdot/f term, which is 3628.

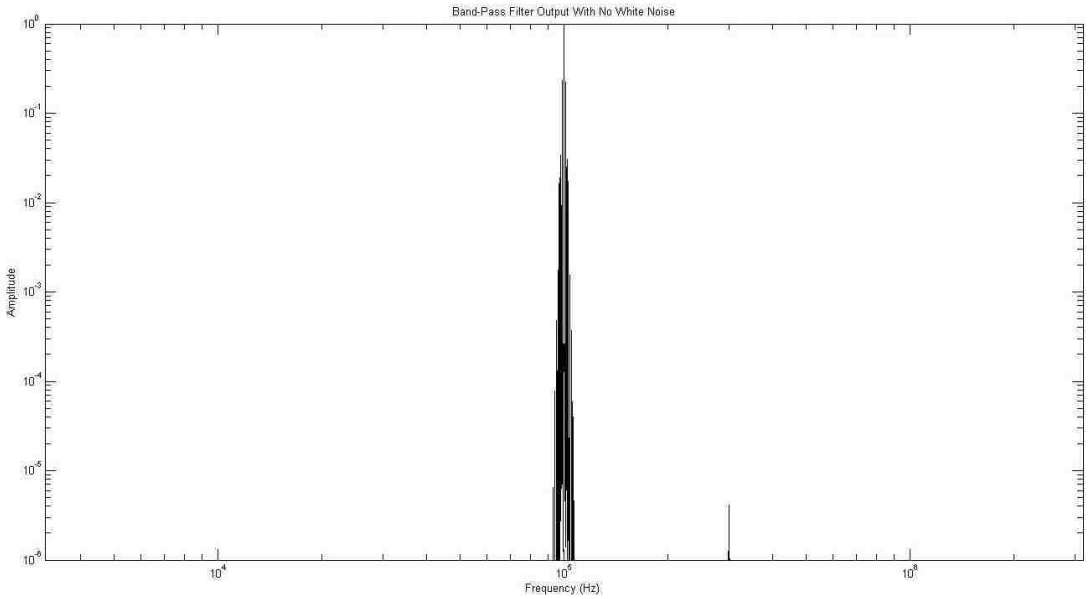

Figure 40: Feedback Noiseless BPF Output DFT 1kHz Sideband

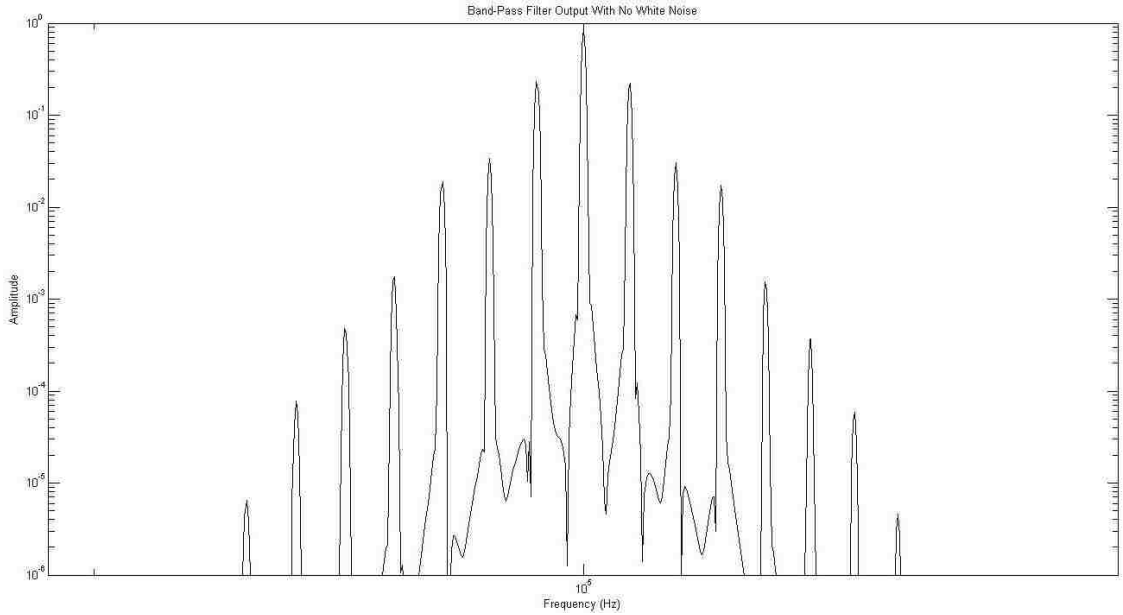

Figure 41: Feedback Noiseless BPF Output DFT 1kHz Sideband Zoomed In

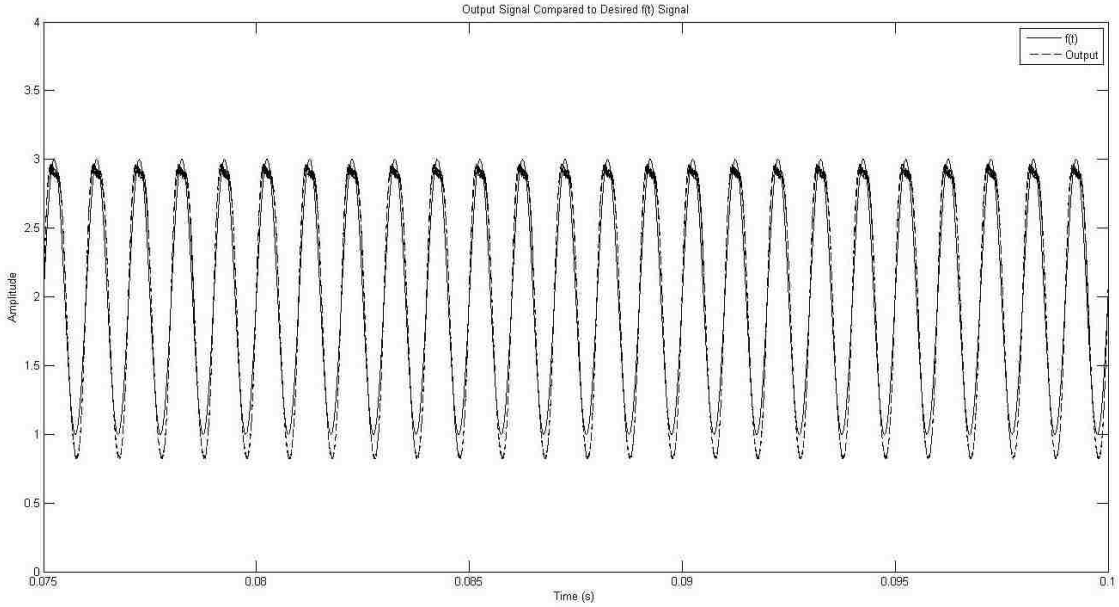

Figure 42: Feedback Noiseless System Output and f(t) Comparison 1kHz Sideband

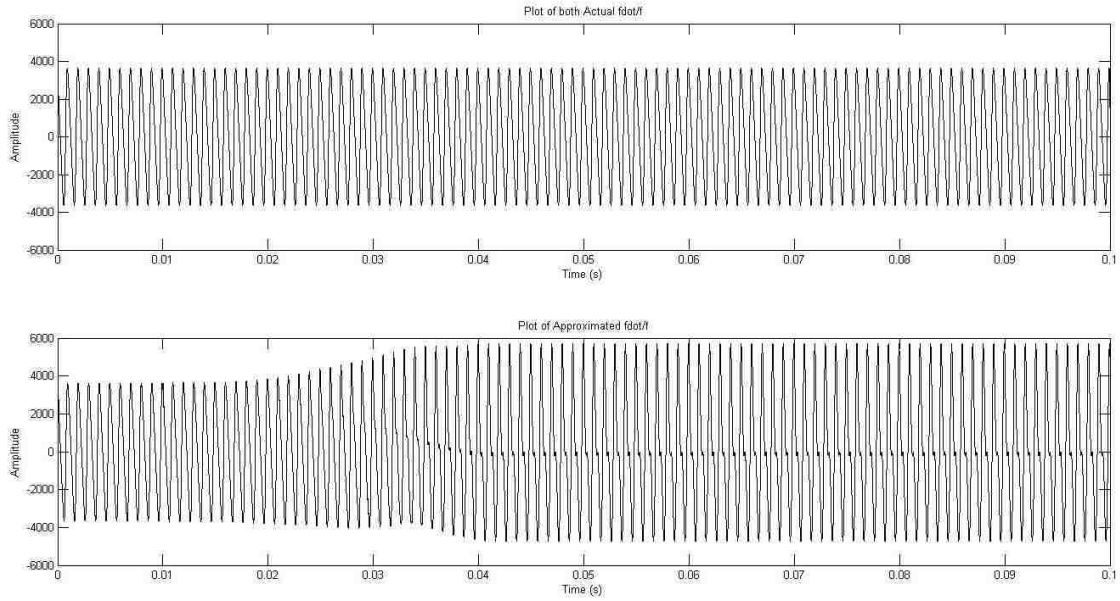

Figure 43: Feedback "fdot/f" Comparison Plots Noiseless 1kHz Sideband

C. Full Feedback System Tested with 1kHz Sidebands and Noise

In the case where noise was added to the input to the band-pass filter, the band-pass filter continued performing properly on noise outside of the cutoff bandwidth. The plot of the noise attenuation can be found in *Figure 44*. In *Figure 45*, the harmonics are experiencing a very similar gain that they did under the circumstances from the noise-free test. In fact, the gain on these sidebands is 14.2%, which is quite close to the noise-free case. The noise acts to further degrade the fdot/f term, as a large portion of the noise spectrum can be fed into the feedback system until the Q-factor ramps up to a high enough level. The output continues to resemble a sinusoidal wave that is very similar to the input f(t), but distortion is also a clear issue. As can be seen in *Figure 47*, the fdot/f term experiences a ramping up process at the same time that the ramp up of the Q-factor occurs.

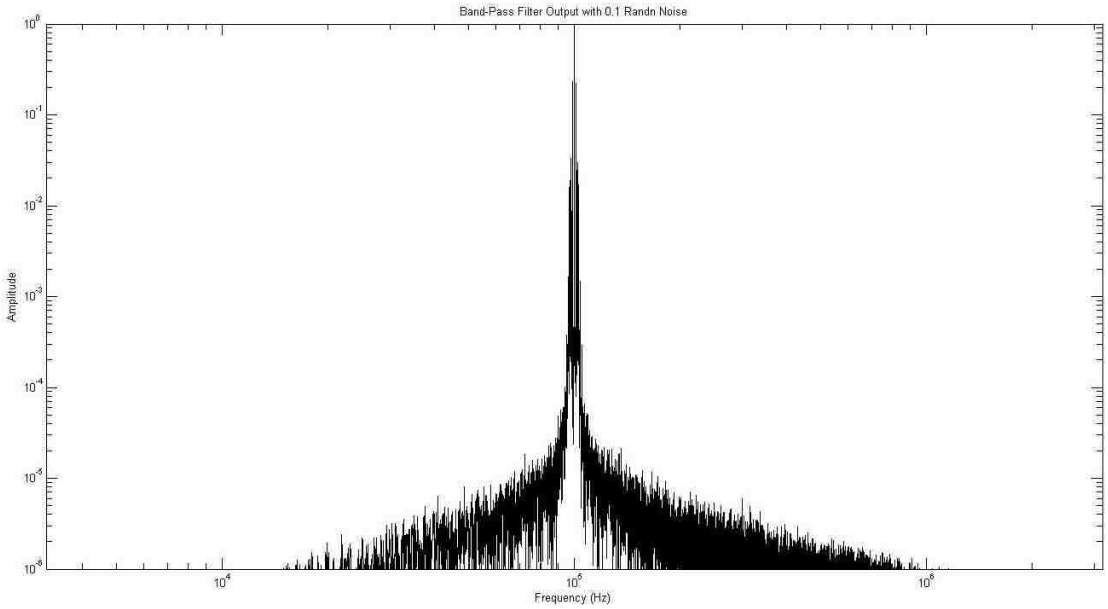

Figure 44: Feedback Noisy BPF Output DFT 1kHz Sideband

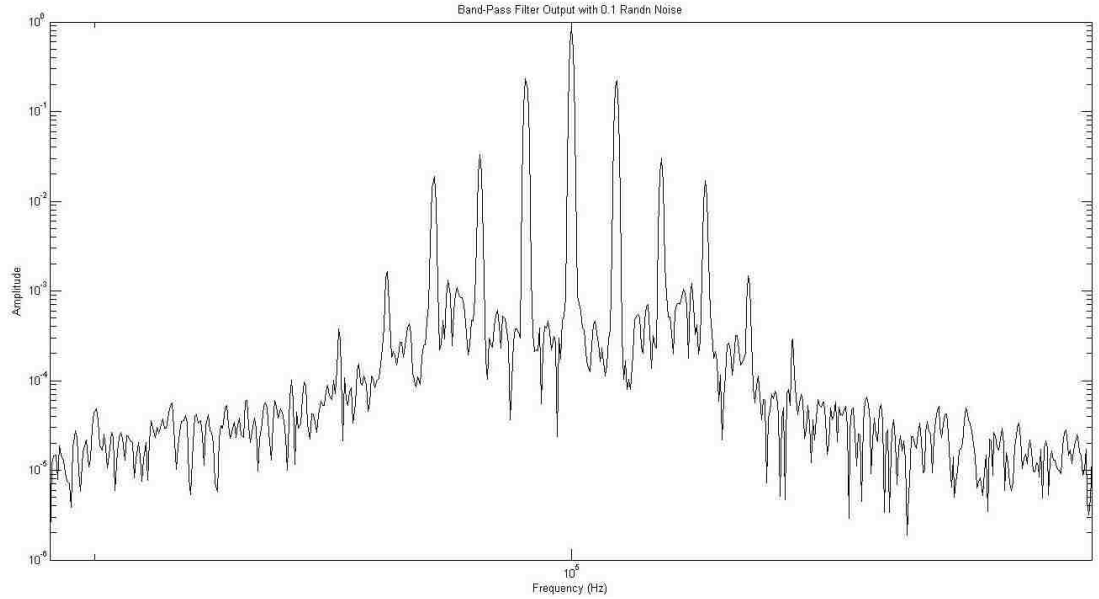

Figure 45: Feedback Noisy BPF Output DFT 1kHz Sideband Zoomed In

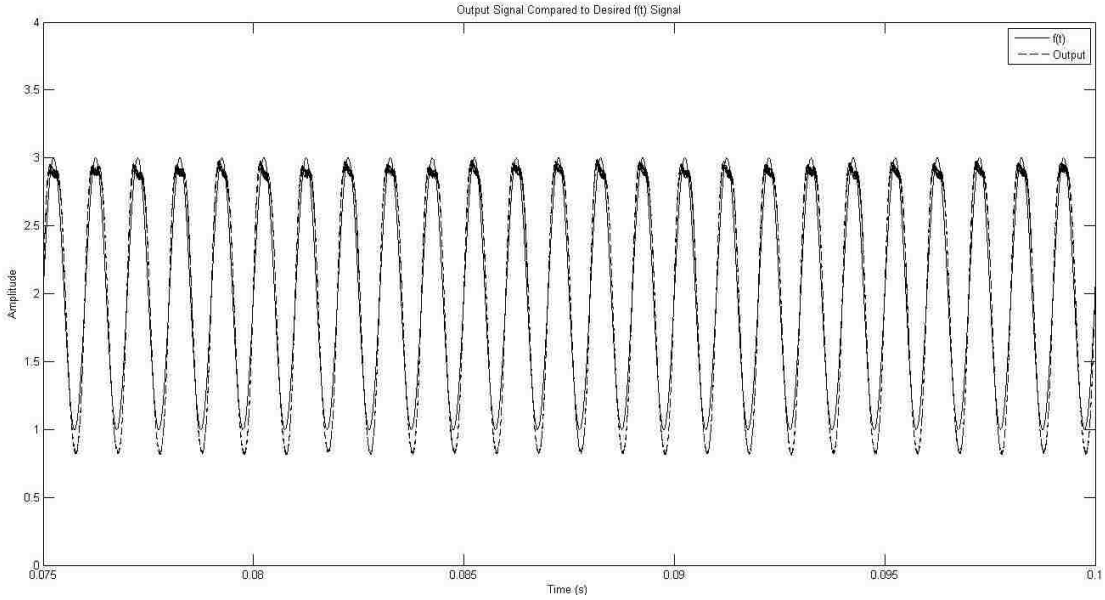

Figure 46: Feedback Noisy System Output and f(t) Comparison 1kHz Sideband

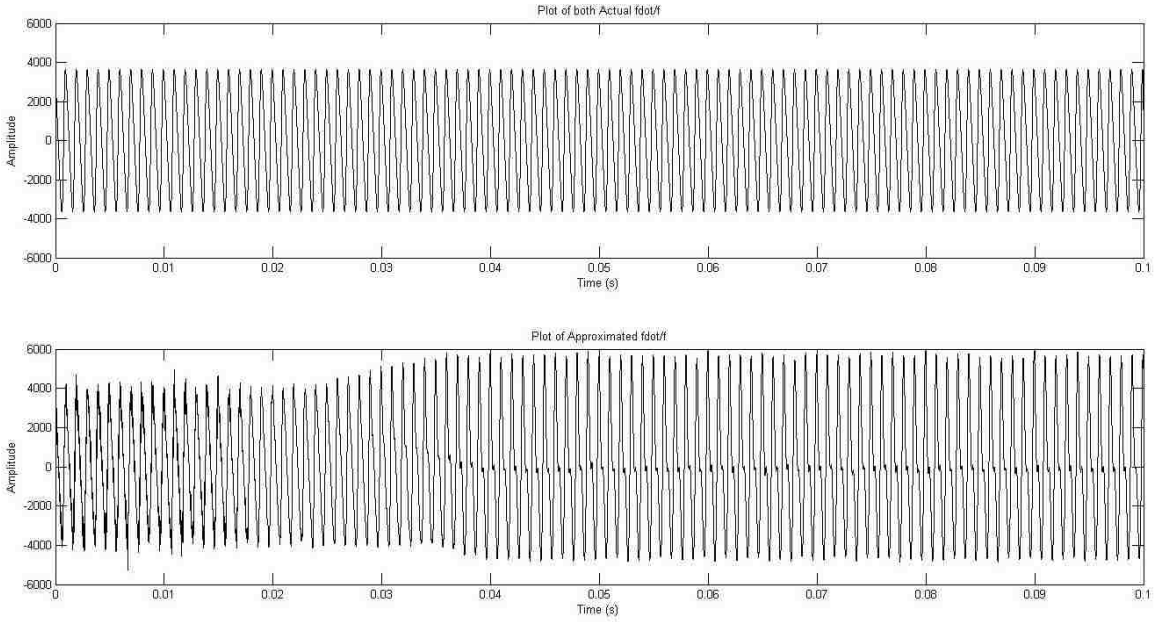

Figure 47: Feedback "fdot/f" Comparison Plots Noisy 1kHz Sideband

D. Full Feedback System Tested with 2kHz Sidebands

A challenge arises when using the 2kHz sidebands with the full feedback system. The fdot/f term that is generated by the feedback system already has some error built in, but when the input f(t) is a higher frequency, the phase shift in the output of the feedback system occurs. This phase shift will cause even more distortion of the signal. This

distortion can be seen in *Figure 48*, where even though no noise is added there is still plenty of distortion. In *Figure 49* it becomes clear something is amiss. The gain of the sidebands has reached 352%, and the harmonic distortion highest peak now reaches 0.1692. The equilibrium of the fdot/f term for this input is not up to par with returning a properly reconstructed signal given the band-pass filter parameters. This gain results in a remarkably large gain at the output of the radio receiver system which can be seen in the time domain plot in *Figure 50*. This is a result of the fdot/f term reaching an equilibrium that has 2.38 times amplitude of the ideal fdot/f term for this f(t).

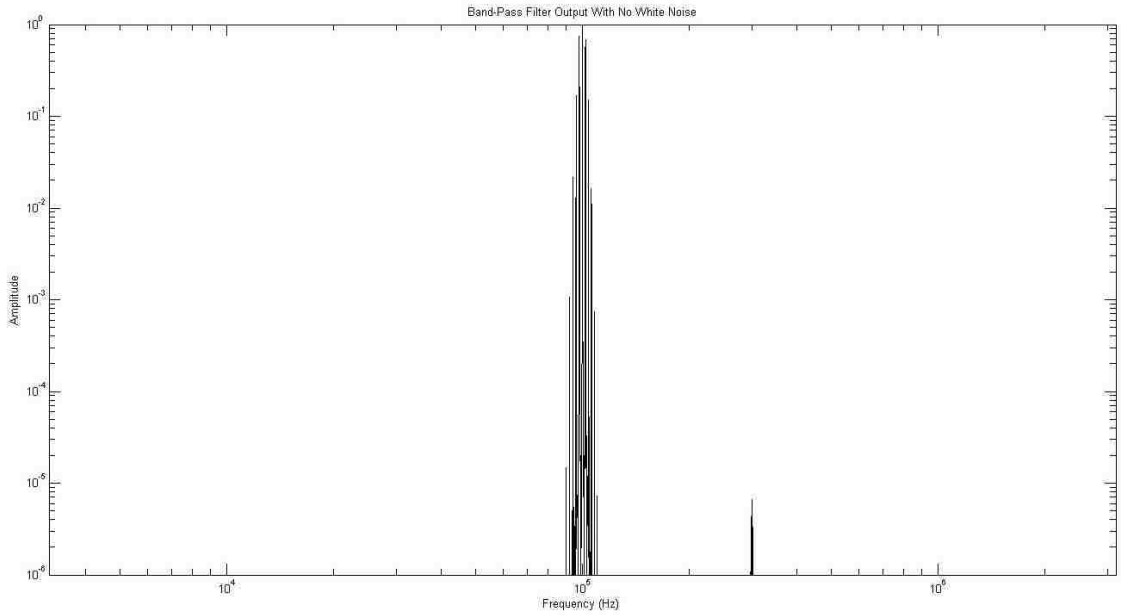

Figure 48: Feedback Noiseless BPF Output DFT 2 kHz Sideband

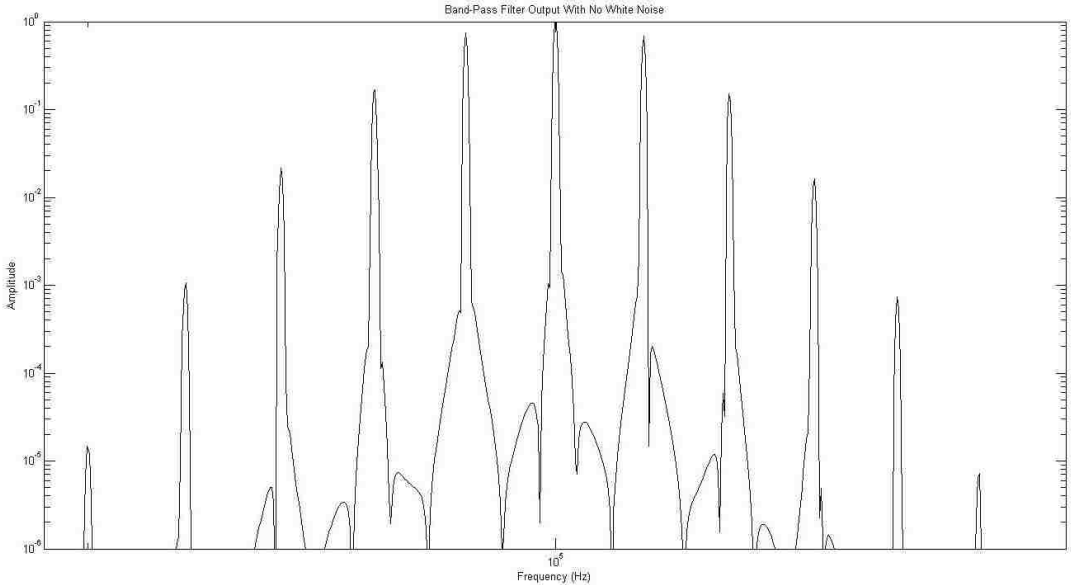

Figure 49: Feedback Noiseless BPF Output DFT 2 kHz Sideband Zoomed In

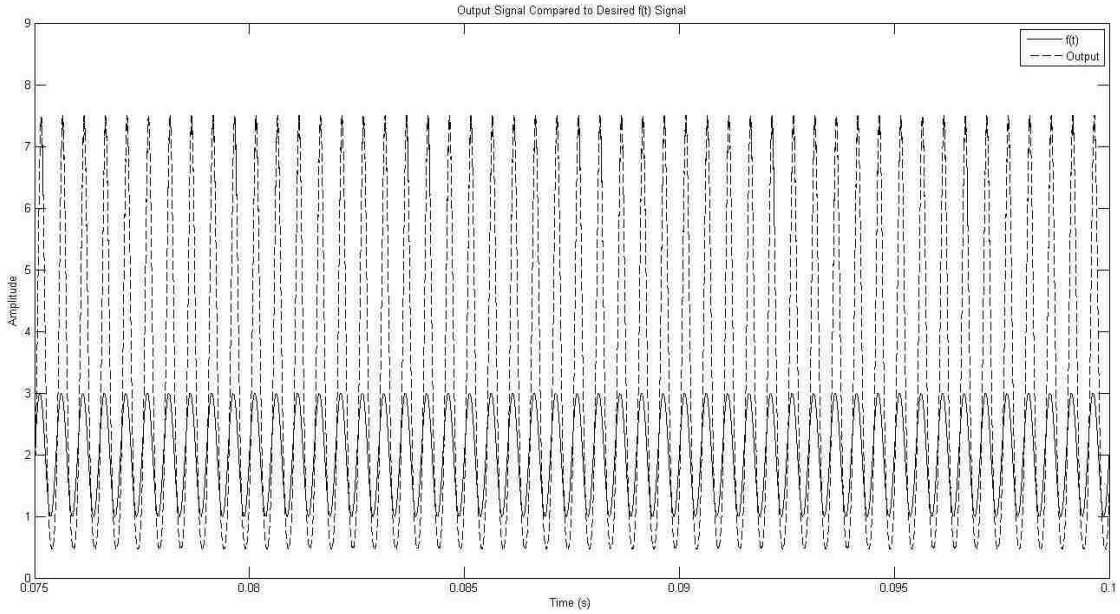

Figure 50: Feedback Noiseless System Output and f(t) Comparison 2kHz Sideband

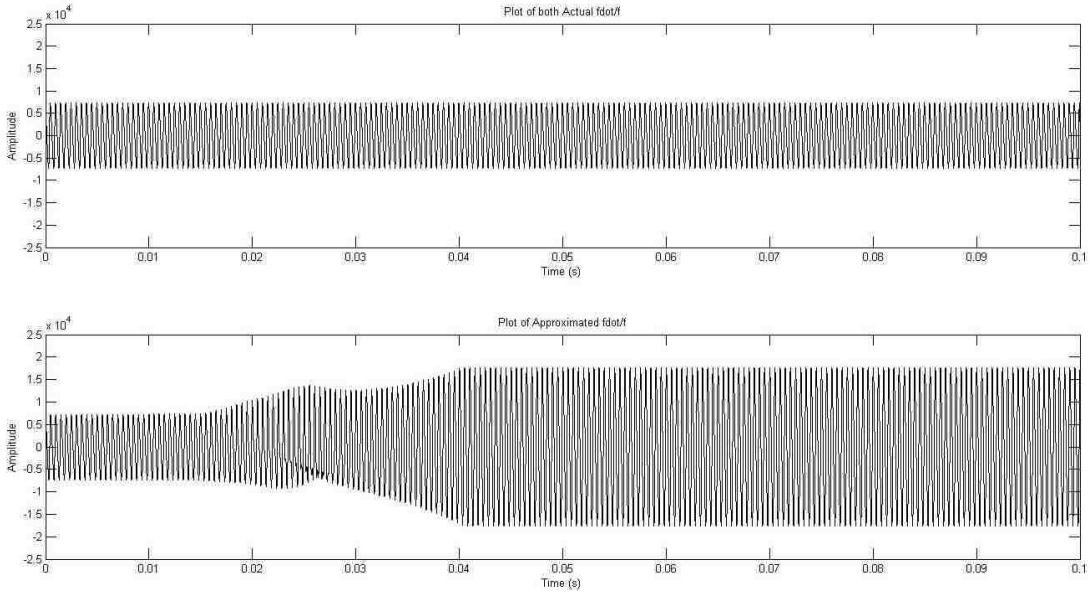

Figure 51: Feedback "fdot/f" Comparison Plots Noiseless 2kHz Sideband

E. Full Feedback System Tested with 2kHz Sidebands and Noise

The added white noise at the input of the band-pass filter can't hide the obvious harmonics which are visible even in *Figure 52*, where the x-axis ranges greatly. The harmonic distortion impulses are being poorly attenuated, and the highest peaks are at 0.1712, which, when compared to the sidebands, is a harmonic distortion of roughly 23%. Just as in the noise-free case, the sidebands are have a significant gain, which is not undesirable in and of itself, but because there is significant distortion in the output, which is shown as a DFT plot in *Figure 53*, and a time-domain plot in *Figure 54*. Also, the fdot/f term is even noisier and more distorted than it was when there was no noise. See *Figure 55* for a plot of fdot/f.

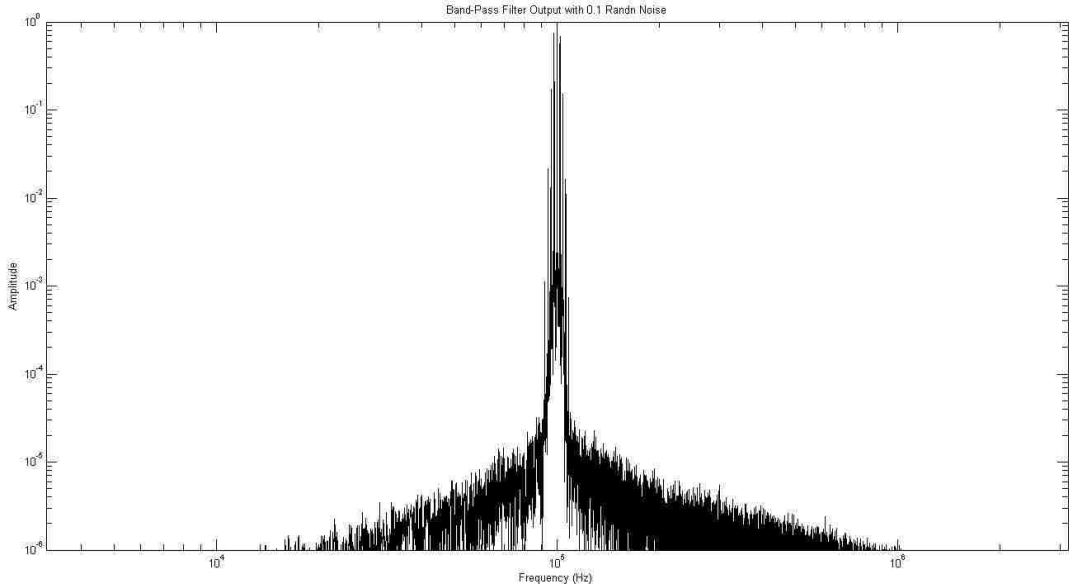

Figure 52: Full Feedback Noisy BPF Output DFT 2

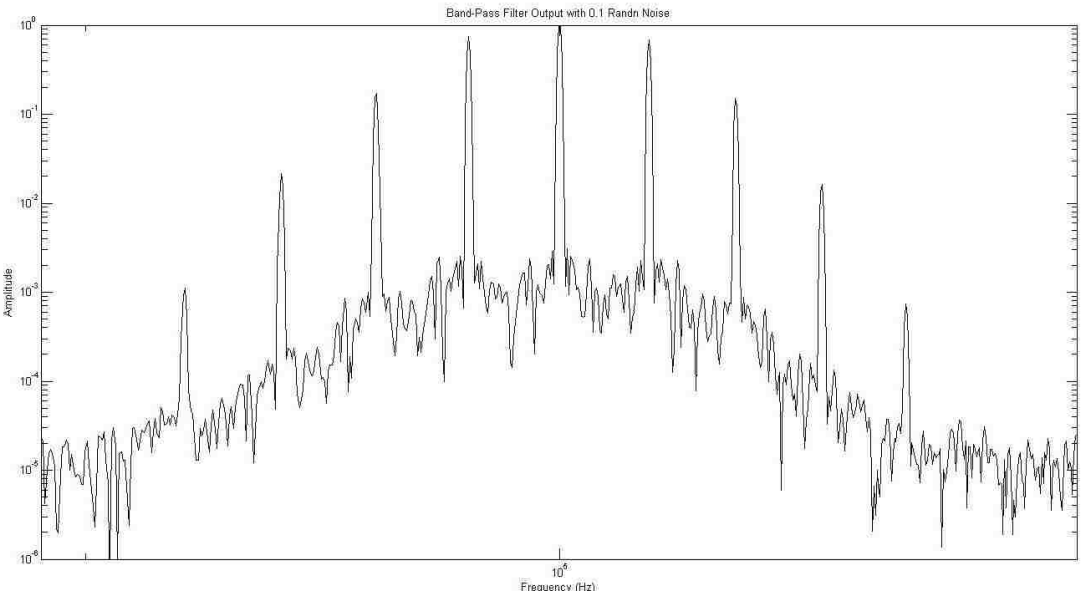

Figure 53: Feedback Noisy BPF Output DFT 2kHz Sideband Zoomed In

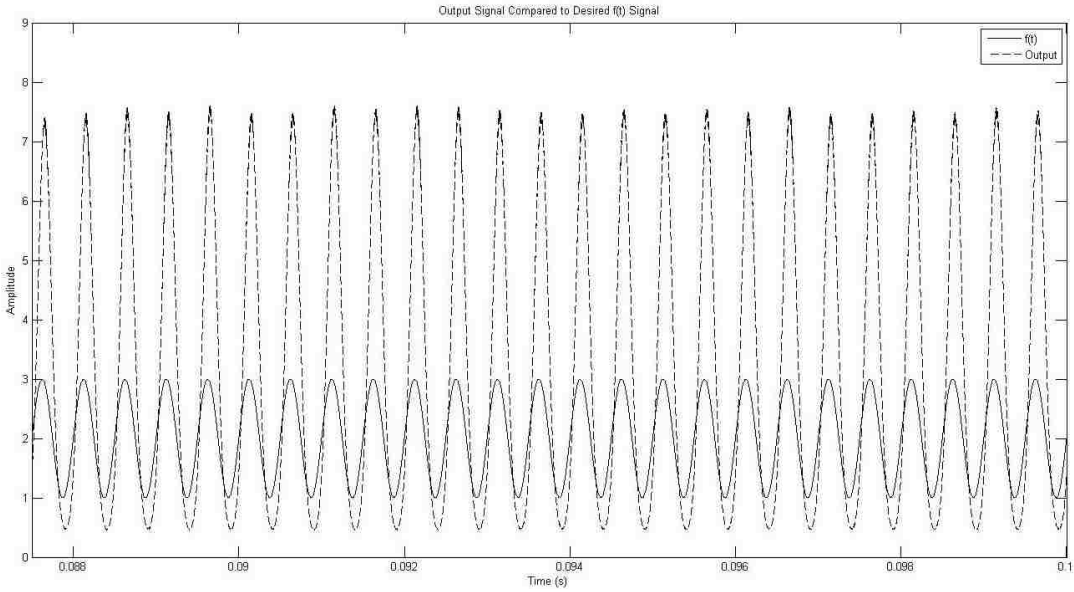

Figure 54: Feedback Noiseless System Output and f(t) Comparison 2kHz Sideband

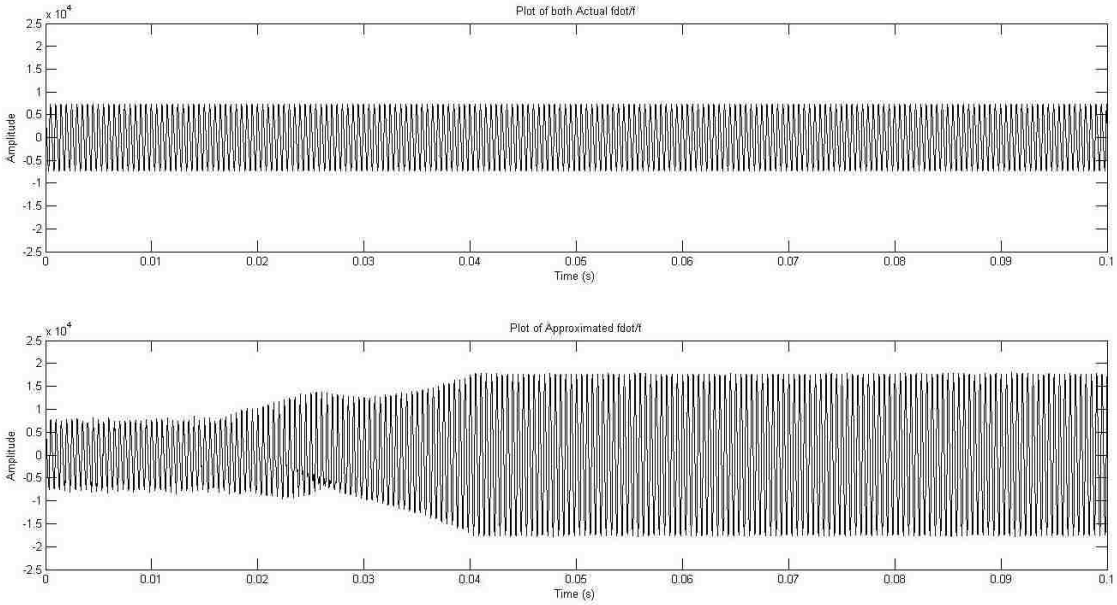

Figure 55: Feedback "fdot/f" Comparison Plots Noisy 2kHz Sideband

VIII. Conclusions

A. Closing Remarks

The different simulations that were run to determine the viability of the claims and assumptions laid out in the introduction were successful in revealing what works

about the system, and what doesn't work. The core concept of the feedback reaching equilibrium where it tries to reconstruct the sidebands of the signal is accurate, and is observable in the results presented in section VII. It was proven through the first set of testing that if the feedback system were to properly provide the band-pass filter with an accurate fdot/f term, the band-pass filter could have a very narrow cutoff bandwidth and still retains the sidebands with very little attenuation. With this, a lower order band-pass filter could be used in place of a higher order one with the same results so long as the designer could develop a filter with a very high Q-factor.

The execution of the feedback system in a closed loop configuration proves that this system can reach a stable equilibrium operation. However, while in the stable equilibrium operation zone, the feedback system has to be generating a very accurate fdot/f term or considerable distortion occurs. A manner must be found in which the feedback system can generate the fdot/f term with almost no phase shift from the true fdot/f term, as phase shift in that term leads to more distortion at the output.

As the simulations progressed, it became clear that for every level of ideality that is stripped away, more error and more needed to be tolerated or designed around. A comparison of the amount of sideband attenuation and the total harmonic distortion at the output of the band-pass filter is given in Table 1.

Table 1: Sideband Attenuation and Total Harmonic Distortion Table

f(t)	Case	Sideband Gain (dB)	Approximate THD
$2 + \sin(2\pi*1000*t)$	Ideal fdot/f, Noiseless	-0.149	0.02%
	Parallel System, Noiseless	+0.423	1.42%
	Feedback System, Noiseless	+0.906	13.30%
	Ideal fdot/f with Noise	-0.140	0.02%
	Parallel System with Noise	+0.457	1.55%
	Feedback System with Noise	+1.152	13%
$2 + \sin(2\pi*2000*t)$	Ideal fdot/f, Noiseless	-0.157	0.03%
	Parallel System, Noiseless	+0.788	1.57%
	Feedback System, Noiseless	+10.930	22.60%
	Ideal fdot/f with Noise	-0.157	0.04%
	Parallel System with Noise	+1.054	1.72%
	Feedback System with Noise	+10.930	23.40%

B. Recommendations for Future Study

It was assumed that the steady state feedback operation for the entire system could reach the proper fdot/f term to fully reconstruct the sidebands with minimal distortion. More research needs to be done to choose a functional block or a modification to the feedback system which can provide more accurate approximations of the fdot/f term with very little phase shift at the output of that feedback system.

References

[1] D. Frey, "Synchronous Filtering", IEEE Trans. on Circuits and Systems—I: Regular Papers, Vol. 53, pp. 1772-1782, August 2006.

[2] K. Martin, "Complex Signal Processing is Not Complex", IEEE Trans on Circuits and Systems, Vol. 51, pp. 1823-1836, September 2004.

[3] C. Thompson, "A Study of Numerical Integration Techniques for Use in the Companion Circuit Method of Transient Analysis", Purdue University E-Publications, April 2004.

[4] S. Franco, Design With Operational Amplifiers and Analog Integrated Circuits, Third Edition, (New York: McGraw-Hill, 1998) 169.

[5] Smith, J.O. Mathematics of the Discrete Fourier Transform (DFT) with Audio Applications, Second Edition, http://ccrma.stanford.edu/~jos/mdft/, 2007, online book, accessed 3 March 2011.

Vita

Kevin Ford was born and raised in Glastonbury, Connecticut, the second of three sons born to Paul and Joyce Ford. A May 2010 graduate, Kevin holds a Bachelor of Science Degree in Mechanical Engineering from Lehigh University with a Minor in Electrical Engineering, and will complete a Master of Science Degree in Electrical Engineering at Lehigh University in May 2011.

As an undergraduate, Kevin won the Alan Stenning award for best undergraduate Mechanical Engineering project, titled "Mechatronic Redesign of a Pinball Machine". Kevin is a member of Phi Beta Kappa Academic Honor Society and of Tau Beta Pi, the Engineering Honor Society.

In addition to his academic pursuits, Kevin is a competitive distance runner who frequently participates in road races ranging from 5 kilometers to half marathon distance.